EUROPEAN ORGANIZATION FOR NUCLEAR RESEARCH (CERN)

CERN-EP-2021-220
2021/11/29

CMS-B2G-20-013

Search for heavy resonances decaying to ZZ or ZW and axion-like particles mediating nonresonant ZZ or ZH production at $\sqrt{s} = 13\,\text{TeV}$

The CMS Collaboration*

Abstract

A search has been performed for heavy resonances decaying to ZZ or ZW and for axion-like particles (ALPs) mediating nonresonant ZZ or ZH production, in final states with two charged leptons ($\ell = \mathrm{e}, \mu$) produced by the decay of a Z boson, and two quarks produced by the decay of a Z, W, or Higgs boson H. The analysis is sensitive to resonances with masses in the range 450 to 1800 GeV. Two categories are defined corresponding to the merged or resolved reconstruction of the hadronically decaying boson. The search is based on data collected during 2016–2018 by the CMS experiment at the LHC in proton-proton collisions at a center-of-mass energy of 13 TeV, corresponding to an integrated luminosity of $138\,\text{fb}^{-1}$. No significant excess is observed in the data above the standard model background expectation. Upper limits on the production cross section of heavy, narrow spin-2 and spin-1 resonances are derived as functions of the resonance mass, and exclusion limits on the production of bulk graviton particles and W′ bosons are calculated in the framework of the warped extra dimensions and heavy vector triplet models, respectively. In addition, upper limits on the ALP-mediated diboson production cross section and ALP couplings to standard model particles are obtained in the framework of linear and chiral effective field theories. These are the first limits on nonresonant ALP-mediated ZZ and ZH production obtained by the LHC experiments.

Submitted to the Journal of High Energy Physics

© 2021 CERN for the benefit of the CMS Collaboration. CC-BY-4.0 license

*See Appendix A for the list of collaboration members

arXiv:2111.13669v1 [hep-ex] 26 Nov 2021

1 Introduction

Several extensions of the standard model (SM) predict the existence of new particles with large couplings to a pair of bosons, either Higgs bosons H or electroweak vector bosons $V = W, Z$. One possibility is the Randall–Sundrum model with warped extra spatial dimensions (WED) [1–3], which predicts heavy spin-2 gravitons (G). Another example is the spin-1 heavy vector triplet (HVT) model [4], which postulates the existence of Z' and W' bosons.

Diboson signatures can also be used to search for axion-like particles (ALPs) [5, 6], designated in this paper by "a". These are neutral pseudoscalar bosons with derivative interactions with SM particles, and often appear in extensions of the SM. Colliders allow for searches in a wide range of ALP masses and couplings [7–9]. An interesting diboson production mechanism is nonresonant ALP-mediated scattering; the ALP is an off-shell mediator in the s-channel $2 \to 2$ scattering processes [9]. Figure 1 shows the Feynman diagrams for the processes $gg \to a^* \to ZZ$ (left) and $gg \to a^* \to ZH$ (right), where a^* is an off-shell ALP. These channels are sensitive to the product of the ALP coupling to gluons and the relevant couplings to dibosons. These channels have been identified as promising because the cross sections are sufficiently large to enable strong constraints to be placed on the theoretical models using the 2016–2018 LHC data set. The derivative interactions enhance the cross section at large diboson invariant masses, $\sqrt{\hat{s}}$. In the ALP off-shell regime $\sqrt{\hat{s}} \gg m_a, m_Z$, where m_a is the ALP mass, the partonic cross section for $gg \to a^* \to ZZ$ varies as $\hat{s}/f_a^4$, where f_a is the energy scale characterizing the new physics. The same type of energy behavior holds for $gg \to a^* \to ZH$. Such energy dependence is only valid as long as the energies probed in the scattering process are smaller than f_a. Factoring in the parton distribution functions (PDFs) of the proton, which tame the energy growth, the differential cross sections for the ALP-mediated processes $pp \to ZZ, ZH$ diminish more slowly as a function of $\sqrt{\hat{s}}$ than for the SM backgrounds. The nonresonant cross sections and kinematical distributions are found to be independent of the ALP mass from arbitrarily light masses up to masses of the order of 100 GeV. The strategy of the search is to look for deviations with respect to the SM expectations in the tails of the experimental diboson mass distributions.

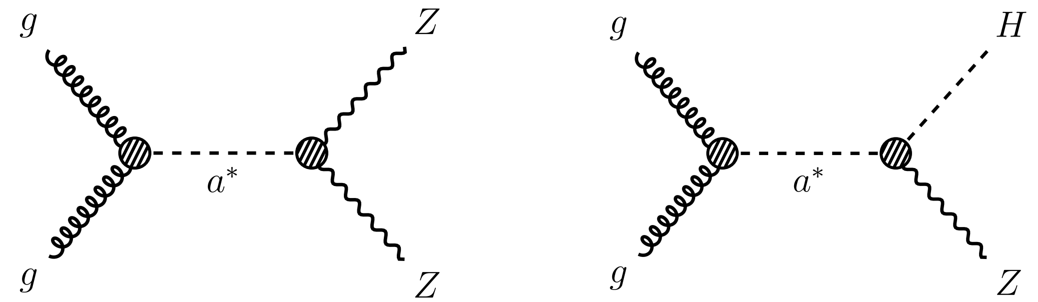

Figure 1: Feynman diagrams for the processes $gg \to ZZ$ (left) and $gg \to ZH$ (right) via an off-shell ALP a^* in the s channel.

This paper reports on the results of a search for spin-2 gravitons decaying to ZZ, spin-1 W' bosons decaying to ZW, and nonresonant ALP-mediated ZZ or ZH production, in final states with two charged leptons ($\ell = e, \mu$) produced by the decay of a Z boson, and two quarks produced by the decay of a Z, W, or Higgs boson. These two quarks can be reconstructed as one single "merged" jet in hadronic decays of a Lorentz-boosted boson, or as two individually resolved jets. The analysis is sensitive to resonances with masses in the range from 450 to 1800 GeV. The width of the heavy resonance is taken to be small in comparison to the experimental resolution [10]. This is the first time a search for the effects of nonresonant ALP-mediated ZZ or ZH production has been performed at the CERN LHC. The search analyzes data collected from 2016 to 2018 by the CMS experiment at $\sqrt{s} = 13\,\text{TeV}$.

Previous searches in similar final states for heavy resonances decaying to two SM bosons at the LHC [11–15] have found no evidence of a signal, providing stringent upper limits on the corresponding production cross sections. Limits on ALP couplings derived from reinterpretations of ATLAS measurements can be found in Ref. [16].

This paper is organized as follows: in Section 2, a description of the signal models, simulated background, and data samples used in the analysis is provided; Section 3 briefly describes the CMS detector; Section 4 provides a description of the event reconstruction; in Section 5, the event selection is discussed; Section 6 describes the estimation of the SM background; the systematic uncertainties affecting the analysis are presented in Section 7; and the results of the search for heavy spin-2 and spin-1 resonances and ALP-mediated diboson production are presented in Section 8. Finally, the results are summarized in Section 9.

Tabulated results are provided in the HEPData record for this analysis [17].

2 Data and simulated samples

This analysis uses data collected with the CMS detector during proton-proton (pp) collisions at the LHC at $\sqrt{s} = 13\,\text{TeV}$, corresponding to an integrated luminosity of $138\,\text{fb}^{-1}$. The events were selected online by criteria that require the presence of at least one electron or muon; these criteria are described in Section 5.

Simulated signal samples are used in the analysis to optimize the search for production of heavy spin-2 and spin-1 resonances, and ALP-mediated ZZ and ZH production. Spin-2 and spin-1 resonant signal samples are generated according to the WED and HVT scenarios, respectively.

In the WED scenario [18, 19], the main free parameters are the mass of the first Kaluza–Klein graviton excitation (the bulk graviton mass) and the ratio $\widetilde{\kappa} = \kappa/\overline{M}_{\text{Pl}}$, where κ is a curvature parameter of the WED metric and $\overline{M}_{\text{Pl}}$ is the reduced Planck mass. The coupling of the bulk graviton to vector bosons is determined by $\widetilde{\kappa}$. Bulk graviton production cross sections, widths, and branching fractions are taken from Ref. [20].

The HVT model [4] introduces a spin-1 triplet of Z′ and W′ bosons. The HVT model generalizes a large number of explicit cases in terms of three parameters: c_{H} determines the coupling to SM vector and Higgs bosons; c_{F} determines the coupling to fermions; and g_{V} is the overall strength of the new vector boson triplet interactions. Benchmark "Model A", with $g_{\text{V}} = 1$, is representative of a model of weakly coupled vector resonances in an extension of the SM gauge group where the HVT bosons have comparable decay branching fractions into SM fermions and vector bosons. Benchmark "Model B", with $g_{\text{V}} = 3$, is representative of a composite model scenario where the HVT boson couplings to fermions are suppressed. The W′ boson production cross sections, widths, and branching fractions are taken from Ref. [4].

For both scenarios, the samples are generated at leading order (LO) in quantum chromodynamics (QCD) with the MadGraph5_aMC@NLO generator [21] versions 2.2.2 (2016) and 2.6.5 (2017 and 2018). Different resonance mass hypotheses are considered in the range 450 to 1800 GeV. Since the resonance width is small in comparison with the experimental resolution, for simplicity, the width is taken to be 1 MeV in the simulation (the narrow-width approximation). The generated spin-2 bulk graviton is forced to decay into two Z bosons, one decaying leptonically into any pair of charged leptons, and the other decaying hadronically into a pair of quarks. In the case of the spin-1 W' boson, the resonance is forced to decay into one Z and one W boson; additionally, the Z boson is then forced to decay to a pair of electrons, muons, or tau leptons, while the W boson is forced to decay into a pair of quarks.

The ALP interactions can be parameterized using the model-independent approach of effective field theories (EFTs). There are two EFT implementations: linear (related to weakly coupled new physics models, with a minimal set of parameters) [22, 23] and chiral (related to strongly coupled new physics models, with more parameters) [24–27]. The ALP couplings to SM particles are proportional to a coefficient c and inversely proportional to the new physics energy scale f_{a}. Here, we adopt the definitions of Refs. [7, 9]. Classical searches for ALPs at colliders consider their couplings to photons and gluons. The coefficient of the gluon coupling is $c_{\widetilde{\mathrm{G}}}$. More recently, interest has extended to consider ALP couplings to electroweak bosons: ZZ, WW, and $\mathrm{Z}\gamma$ [7]. At LO in the linear model, all these and the coupling to photons are related by gauge symmetry to two basic electroweak couplings: $c_{\widetilde{\mathrm{W}}}$ and $c_{\widetilde{\mathrm{B}}}$. The coupling of the ALP to ZZ is $c_{\widetilde{\mathrm{Z}}} = c_{\widetilde{\mathrm{W}}}\, c_w^2 + c_{\widetilde{\mathrm{B}}}\, s_w^2$, where c_w and s_w denote the cosine and sine of the Weinberg angle, respectively. In this analysis, small couplings of the ALP to fermions are set to zero. In the chiral model, the ALP still couples to gluons with coupling $c_{\widetilde{\mathrm{G}}}$. Additionally, the ALP couples to ZH, and there are several coefficients contributing to the ZH vertex [7]. For simplicity, in this chiral analysis, the ALP to ZH coupling coefficient $\widetilde{a}_{2\mathrm{D}}$ is studied; small couplings of the ALP to fermions are neglected and the ZZ channel is considered closed. In both the linear and chiral implementations, interference between the SM and ALP-mediated processes is neglected.

Simulated signals of ALP-mediated production are generated with MADGRAPH5_aMC@NLO 2.6.5 using both the linear and chiral EFT models [7]. In the linear model, $\mathrm{gg} \to \mathrm{a}^* \to \mathrm{ZZ}$ events are generated at LO with $c_{\widetilde{\mathrm{G}}}/f_{\mathrm{a}} = c_{\widetilde{\mathrm{Z}}}/f_{\mathrm{a}} = 1\,\mathrm{TeV}^{-1}$ and an ALP mass of 1 MeV. The MADGRAPH5_aMC@NLO cross sections are 77 (92, 94, 95) pb for $\sqrt{\hat{s}} < f_{\mathrm{a}} = 1$ (2, 3, 7) TeV, respectively. One Z boson is forced to decay leptonically and the other hadronically. In the chiral model, $\mathrm{gg} \to \mathrm{a}^* \to \mathrm{ZH}$ events are generated at LO with $c_{\widetilde{\mathrm{G}}}/f_{\mathrm{a}} = \widetilde{a}_{2\mathrm{D}}/f_{\mathrm{a}} = 1\,\mathrm{TeV}^{-1}$ and an ALP mass of 1 MeV; all other chiral coefficients are set to zero. The MADGRAPH5_aMC@NLO cross sections are 63 (78, 80, 81) pb for $\sqrt{\hat{s}} < f_{\mathrm{a}} = 1$ (2, 3, 7) TeV, respectively. The Z boson is forced to decay leptonically; the Higgs boson is decayed according to the branching fractions predicted in the SM. In both cases, there is a 7% systematic uncertainty in the size of the cross sections related to the renormalization and factorization scales, and a 1.2% systematic uncertainty related to the PDFs.

Several SM processes yielding final states with charged leptons and jets are sources of background events for the analysis, and corresponding Monte Carlo simulated samples have been generated to study them.

The SM production of a Z boson in association with quarks or gluons in the final state ($\mathrm{Z}+\mathrm{jets}$) represents the dominant background process for the analysis, having topological similarities to the signal because of the presence of a pair of charged leptons and jets. However, since the quark- and gluon-induced jets are not associated with the decay of a vector boson, the merged-jet and dijet mass spectra are characterized by smooth distributions, and the distribution of the $2\ell 2\mathrm{q}$ system invariant mass falls exponentially. In contrast, the signals are expected to have peaking distributions in the merged-jet and dijet mass spectra, and a distinctive $2\ell 2\mathrm{q}$ mass distribution. The simulated $\mathrm{Z}+\mathrm{jets}$ samples are produced with MADGRAPH5_aMC@NLO at next to LO (NLO) for 2016 samples, and LO for 2017 and 2018 samples. Both LO and NLO sample events are reweighted to account for electroweak NLO corrections, with the LO events also reweighted for QCD NLO corrections [28].

The SM diboson production of ZV and ZH is an irreducible source of background for the analysis, since the merged-jet and dijet mass spectra will contain a peak from the hadronic decay of H, W, and Z bosons; however, this process produces a smoothly falling $2\ell 2q$ invariant mass distribution. The SM production of pairs of bosons (ZZ, ZW, and ZH) is simulated at NLO with MADGRAPH5_aMC@NLO.

The parton showering and hadronization is simulated by interfacing the event generators with PYTHIA 8.226 [29] with the CUETP8M1 [30] tune for 2016 resonant samples and backgrounds, and PYTHIA 8.230 with the CP5 [31] tune for 2017 and 2018 resonant samples and backgrounds. The CUETP8M1 tune is used with PYTHIA 8.230 for all ALP simulated samples. The PDFs of the colliding protons are given by the NNPDF 3.0 [32] PDF set for 2016 resonant samples and backgrounds, and the NNPDF 3.1 [33] set for 2017 and 2018 resonant samples and backgrounds, as well as all ALP simulated samples. Additional pp interactions occurring in the same or nearby bunch crossings (pileup) are added to the event simulation, with a frequency distribution adjusted to match that observed in data. All samples are processed through a simulation of the CMS detector using GEANT4 [34] and reconstructed using the same algorithms as those for analysis of the data.

3 The CMS detector

The central feature of the CMS apparatus is a superconducting solenoid of 6 m internal diameter, providing a magnetic field of 3.8 T. Within the solenoid volume are a silicon pixel and strip tracker, a lead tungstate crystal electromagnetic calorimeter (ECAL), and a brass and scintillator hadron calorimeter (HCAL), each composed of a barrel and two endcap sections. Forward calorimeters extend the pseudorapidity η coverage provided by the barrel and endcap detectors. Muons are measured in gaseous detectors embedded in the steel flux-return yoke outside the solenoid.

Events of interest are selected using a two-tiered trigger system. The first level, composed of custom hardware processors, uses information from the calorimeters and muon detectors to select events at a rate of around 100 kHz within a fixed latency of about 4 μs [35]. The second level, known as the high-level trigger, consists of a farm of processors running a version of the full event reconstruction software optimized for fast processing, and reduces the event rate to around 1 kHz before data storage [36].

A more detailed description of the CMS detector, together with a definition of the coordinate system used and the relevant kinematic variables, can be found in Ref. [37].

4 Event reconstruction

The particle-flow (PF) algorithm [38] aims to reconstruct and identify each individual particle in an event, with an optimized combination of information from the various elements of the CMS detector. The energy of photons is obtained from the ECAL measurement. The energy of electrons is determined from a combination of the electron momentum at the primary interaction vertex as determined by the tracker, the energy of the corresponding ECAL cluster, and the energy sum of all bremsstrahlung photons spatially compatible with originating from the electron track. The energy of muons is obtained from the curvature of the corresponding track. The energy of charged hadrons is determined from a combination of their momentum measured in the tracker and the matching ECAL and HCAL energy deposits, corrected for the response function of the calorimeters to hadronic showers. Finally, the energy of neutral hadrons is obtained from the corresponding corrected ECAL and HCAL energies.

The candidate vertex with the largest value of summed physics-object p_T^2, where p_T is the transverse momentum, is taken to be the primary pp interaction vertex. The physics objects are the jets, clustered using the jet finding algorithm [39, 40] with the tracks assigned to candidate vertices as inputs, and the associated missing p_T, taken as the negative vector sum of the p_T of those jets.

The silicon tracker used in 2016 measured charged particles within the range $|\eta| < 2.5$. For nonisolated particles of $1 < p_T < 10$ GeV and $|\eta| < 1.4$, the track resolutions are typically 1.5% in p_T and 25–90 (45–150) μm in the transverse (longitudinal) impact parameter [41]. At the start of 2017, the tracker was upgraded [42] to measure up to $|\eta| < 3.0$; the resolutions of the upgraded tracker were typically 1.5% in p_T and 20–75 μm in the transverse impact parameter [43] for nonisolated particles of $1 < p_T < 10$ GeV and $|\eta| < 3.0$.

The electron momentum is estimated by combining the energy measurement in the ECAL with the momentum measurement in the tracker. The momentum resolution for electrons with $p_T \approx 45$ GeV from $Z \rightarrow ee$ decays ranges from 1.7 to 4.5%. It is generally better in the barrel region than in the endcaps, and also depends on the bremsstrahlung energy emitted by the electron as it traverses the material in front of the ECAL [44].

Muons are measured in the range $|\eta| < 2.4$, with detection planes made using three technologies: drift tubes, cathode strip chambers, and resistive-plate chambers. The single-muon trigger efficiency exceeds 90% over the full η range, and the efficiency to reconstruct and identify muons is greater than 96%. Matching muons to tracks measured in the silicon tracker results in a relative p_T resolution, for muons with p_T up to 100 GeV, of 1% in the barrel and 3% in the endcaps, and of better than 7% for muons in the barrel with p_T up to 1 TeV [45].

Both electrons and muons are required to be isolated from hadronic activity and other leptons in the event. An isolation variable is defined as the scalar sum of the p_T of charged hadrons originating from the primary vertex, plus the scalar sums of the p_T for neutral hadrons and photons, in a cone of $\Delta R = \sqrt{(\Delta\eta)^2 + (\Delta\phi)^2} < 0.3\,(0.4)$ around the electron (muon) direction, where ϕ is the azimuthal angle, corrected to account for the contribution from neutral candidates originating from pileup [44, 45].

Hadronic jets are clustered from particles reconstructed by the PF algorithm using the infrared- and collinear-safe anti-k_T algorithm [39, 40] with distance parameters of 0.4 (AK4 jets) and 0.8 (AK8 jets). The jet momentum is determined as the vectorial sum of all particle momenta in the jet, and is found from simulation to be, on average, within 5–10% of the true momentum over the entire p_T spectrum and detector acceptance. For AK4 jets, contamination from pileup is suppressed using charged-hadron subtraction, which removes from the list of PF candidates all charged particles originating from vertices other than the primary interaction vertex of the event. The residual contribution from neutral particles originating from pileup vertices is removed by means of an event-by-event jet-area-based correction to the jet four-momentum [46]. For AK8 jets, the pileup per particle identification algorithm (PUPPI) [47] is used to mitigate the effect of pileup at the reconstructed particle level, making use of local shape information, event pileup properties, and tracking information.

Jet energy corrections are derived from simulation studies so that the average measured energy of jets becomes identical to that of particle-level jets. In situ measurements of the momentum balance in dijet, photon + jet, Z + jet, and multijet events are used to determine any residual differences between the jet energy scale in data and in simulation, and appropriate corrections are made [10]. Additional selection criteria are applied to each jet to remove jets potentially dominated by instrumental effects or reconstruction failures [48].

A jet grooming technique is used for AK8 jets in this analysis to help identify and discriminate between merged jets from hadronic decays of boosted V and Higgs bosons, and jets from quarks and gluons. The AK8 jets are groomed by means of the modified mass drop tagger algorithm [49], also known as the soft-drop algorithm, with angular exponent $\beta = 0$, soft cutoff threshold $z_{\text{cut}} < 0.1$, and characteristic radius $R_0 = 0.8$ [50]. The soft-drop algorithm does not fully reject contributions from the underlying event and pileup. The mass of the AK8 jet (m_{J}) is therefore defined as the invariant mass associated to the four-momentum of the soft-drop jet, after the PUPPI corrections are applied.

Discrimination between AK8 jets originating from vector boson decays and those originating from gluons and quarks is further improved by the N-subjettiness jet substructure variable [51]. This observable exploits the distribution of the jet constituents found in the proximity of the subjet axes to determine if the jet can be effectively subdivided into a number N of subjets. The generic N-subjettiness variable τ_N is defined as the p_{T}-weighted sum of the angular distance of all the k jet constituents from the closest subjet:

$$\tau_N = \frac{1}{d_0} \sum_k p_{\text{T},k} \min(\Delta R_{1,k}, \Delta R_{2,k}, \ldots, \Delta R_{N,k}). \tag{1}$$

The normalization factor d_0 is defined as $d_0 = \sum_k p_{\text{T},k} R_{\text{j}}$, with R_{j} the clustering parameter of the original jet. In this analysis, which aims to select $\text{V} \to \text{qq}$ decays, the variable that best discriminates between V boson jets and those from quarks and gluons is the ratio of the 2-subjettiness to 1-subjettiness: $\tau_{21} = \tau_2/\tau_1$. The τ_{21} observable is calculated for the jet before the grooming procedure, and includes the PUPPI algorithm corrections for pileup mitigation.

For the identification of jets originating from the hadronization of bottom quarks, the deep neural network-based combined secondary vertex (DEEPCSV) algorithm [52] is used, either directly on the AK4 jets or on the AK8 soft-drop subjets with PUPPI pileup mitigation applied. A DEEPCSV loose (medium) b tag corresponds to a ≈84 (≈68)% efficiency for b quark identification and a ≈10 (≈1)% light-flavor or gluon jet mistag rate.

Jets are required to be separated from isolated leptons by $\Delta R > 0.8\,(0.4)$ for AK8 (AK4) jets. Only those AK4 and AK8 jets passing the tight jet identification requirements [48], and reconstructed in the central region of the detector ($|\eta| < 2.4$), are considered in the analysis.

5 Event selection

In the online selection, events must satisfy either a single-electron or a single-muon trigger. The electron trigger requires either an electron with $p_{\text{T}} > 27\,(32)$ GeV and $|\eta| < 2.4$ in the 2016 (2017 and 2018) data sample, passing tight identification and isolation requirements, or an electron with $p_{\text{T}} > 115$ GeV and $|\eta| < 2.4$ with no isolation requirements. The muon trigger requires a muon with $p_{\text{T}} > 24\,(27)$ GeV and $|\eta| < 2.4$ in 2016 and 2018 (2017), passing loose identification and isolation requirements.

In the offline selection, two well-identified leptons are first required. The leading and subleading leptons are required to have $p_{\text{T}} > 40$ GeV in the range $|\eta| < 2.4$. Electrons (muons) must satisfy tight identification and tight (loose) isolation requirements. Reconstruction, identification, and isolation efficiencies for leptons and their uncertainties are evaluated from dedicated data samples of leptonic Z boson decays, where one lepton from the decay serves as a tag and the efficiency for the other lepton is measured [53]. A leptonic Z candidate is defined as a pair of leptons with the same flavor, opposite charges, and invariant mass $76 < m_{\ell\ell} < 106\,\text{GeV}$.

Depending on the boson p_{T} in $\mathrm{V} \to \mathrm{q\overline{q}}$ and $\mathrm{H} \to \mathrm{q\overline{q}}$ decays, the decay products may either be reconstructed as a single AK8 merged jet (boosted category) or as a pair of AK4 jets (resolved category). In the following, j refers to AK4 jets and J refers to AK8 jets.

In the boosted selection, events must have a leptonic Z candidate with $p_{\mathrm{T}}(\ell\ell) > 200\,\text{GeV}$ and one AK8 jet with $p_{\mathrm{T}}(\mathrm{J}) > 200\,\text{GeV}$ and soft-drop mass $m_{\mathrm{J}} > 30\,\text{GeV}$. If several AK8 jets in the event satisfy the requirements, the one with the highest p_{T} is considered. Boosted hadronic V and H candidates are first defined by $\tau_{21} < 0.40\,(0.45)$ in 2016 (2017 and 2018), and then by the soft-drop mass signal regions $65 < m_{\mathrm{J}} < 105\,\text{GeV}$ (SR1) and $95 < m_{\mathrm{J}} < 135\,\text{GeV}$ (SR2), respectively. Figure 2 shows the τ_{21} and merged $p_{\mathrm{T}}(\mathrm{J})$ distributions for boosted hadronic V and H candidates. In addition, boosted hadronic sideband (SB) candidates are defined by the τ_{21} requirement and the soft-drop mass regions $30 < m_{\mathrm{J}} < 65\,\text{GeV}$ and $135 < m_{\mathrm{J}} < 300\,\text{GeV}$.

In the resolved selection, boosted events are vetoed; events must have a leptonic Z candidate with $p_{\mathrm{T}}(\ell\ell) > 150\,\text{GeV}$ and an AK4 dijet system with $p_{\mathrm{T}}(\mathrm{j}) > 30\,\text{GeV}$, $p_{\mathrm{T}}(\mathrm{jj}) > 150\,\text{GeV}$, $m_{\mathrm{jj}} > 30\,\text{GeV}$, and $\Delta R(\mathrm{jj}) < 1.5$. In events with more than two AK4 jets, the best dijet combination is chosen based on the following criteria: the dijet in the highest b tag category is first selected; if more than one dijet combination remains, the pair closest in mass to the target signal boson is chosen. Resolved hadronic V and H candidates are defined by the dijet mass signal regions $65 < m_{\mathrm{jj}} < 110\,\text{GeV}$ (SR1) and $95 < m_{\mathrm{jj}} < 135\,\text{GeV}$ (SR2), respectively. In addition, resolved hadronic SB candidates are defined by the dijet mass regions $30 < m_{\mathrm{jj}} < 65\,\text{GeV}$ and $135 < m_{\mathrm{jj}} < 180\,\text{GeV}$.

Boosted (resolved) events belong to the tagged category if the hadronic V or H candidate contains one subjet (jet) with a medium b tag and the other subjet (jet) with a loose b tag. Otherwise, they are placed in the untagged category. Figure 3 shows the distributions of the untagged and loose and medium DEEPCSV tags for subjets of the boosted hadronic H candidates in SR2.

In total, eight categories are defined by the combination of electrons/muons, boosted/resolved, and tagged/untagged. Table 1 summarizes the selection and categorization requirements of the analysis. Figure 4 shows the merged jet m_{J} and dijet m_{jj} distributions for the untagged and tagged categories in the signal and sideband regions.

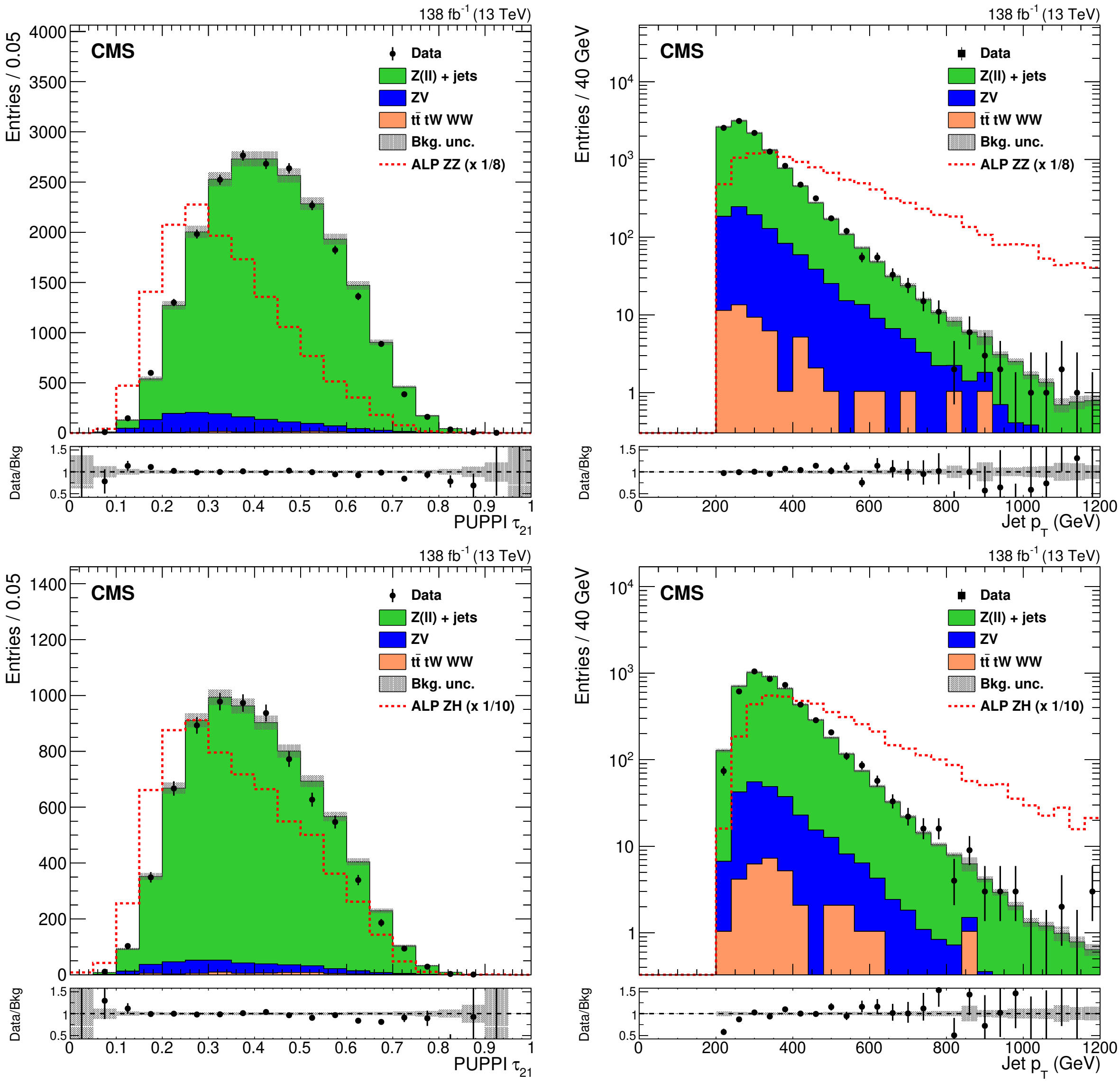

Figure 2: Distributions of the merged jet τ_{21} (left) and p_{T} after applying the τ_{21} selection (right) for boosted hadronic V (upper) and H (lower) candidates. The gray band shows the statistical and systematic uncertainties in the background. The background for the τ_{21} distributions is normalized to the number of events in the data; the background normalization for the jet p_{T} distributions is derived from the final fit to the data. The red dashed histograms correspond to a hypothetical linear (chiral) ALP with 1 TeV^{-1} couplings to gluons and ZZ (ZH), and $f_{\mathrm{a}} = 3$ TeV; the cross sections have been multiplied by the factors indicated in the legends for better visibility. The lower panels show the ratio of data to background.

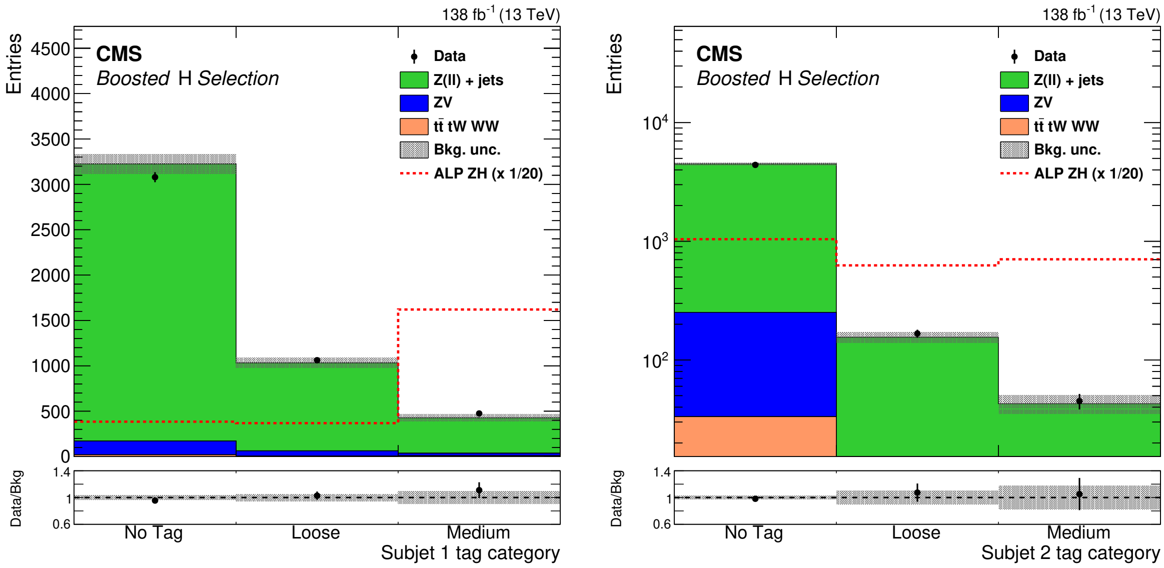

Figure 3: Distributions of the untagged and loose and medium DEEPCSV tags for the more b-like subjet (left) and the less b-like subjet (right) of the boosted hadronic H candidates in SR2. The gray band shows the statistical and systematic uncertainties in the background. Background normalizations are derived from the final fit to the data. The red dashed histograms correspond to a hypothetical chiral ALP with 1 TeV^{-1} couplings to gluons and ZH, and $f_a = 3$ TeV; the cross sections have been multiplied by the factors indicated in the legends for better visibility. The lower panels show the ratio of data to background.

Table 1: Summary of selection requirements and categorization.

Observable	Event category: Resolved	Event category: Boosted
Leptons	Same flavor, opposite charge	
$p_T(\ell)$ (GeV)	>40	>40
$\lvert\eta(\ell)\rvert$	<2.4	<2.4
$m_{\ell\ell}$ (GeV)	[76, 106]	[76, 106]
$\lvert\eta(j)\rvert$ or $\lvert\eta(J)\rvert$	<2.4	<2.4
$\Delta R(\ell J)$ (AK8)	—	>0.8
$\Delta R(\ell j)$ (AK4)	>0.4	—
$\Delta R(jj)$	<1.5	—
$p_T(\ell\ell)$ (GeV)	>150	>200
$p_T(jj)$ or $p_T(J)$ (GeV)	>150	>200
PUPPI τ_{21}	—	<0.4 (2016), <0.45 (2017, 2018)
SR1 m_{jj} or m_J (GeV)	[65, 110]	[65, 105]
SR2 m_{jj} or m_J (GeV)	[95, 135]	[95, 135]
SB m_{jj} or m_J (GeV)	[30, 65] ⋃ [135, 180]	[30,65] ⋃ [135,300]
b tagging	Untagged / Tagged [L+M]	Untagged / Tagged [L+M]

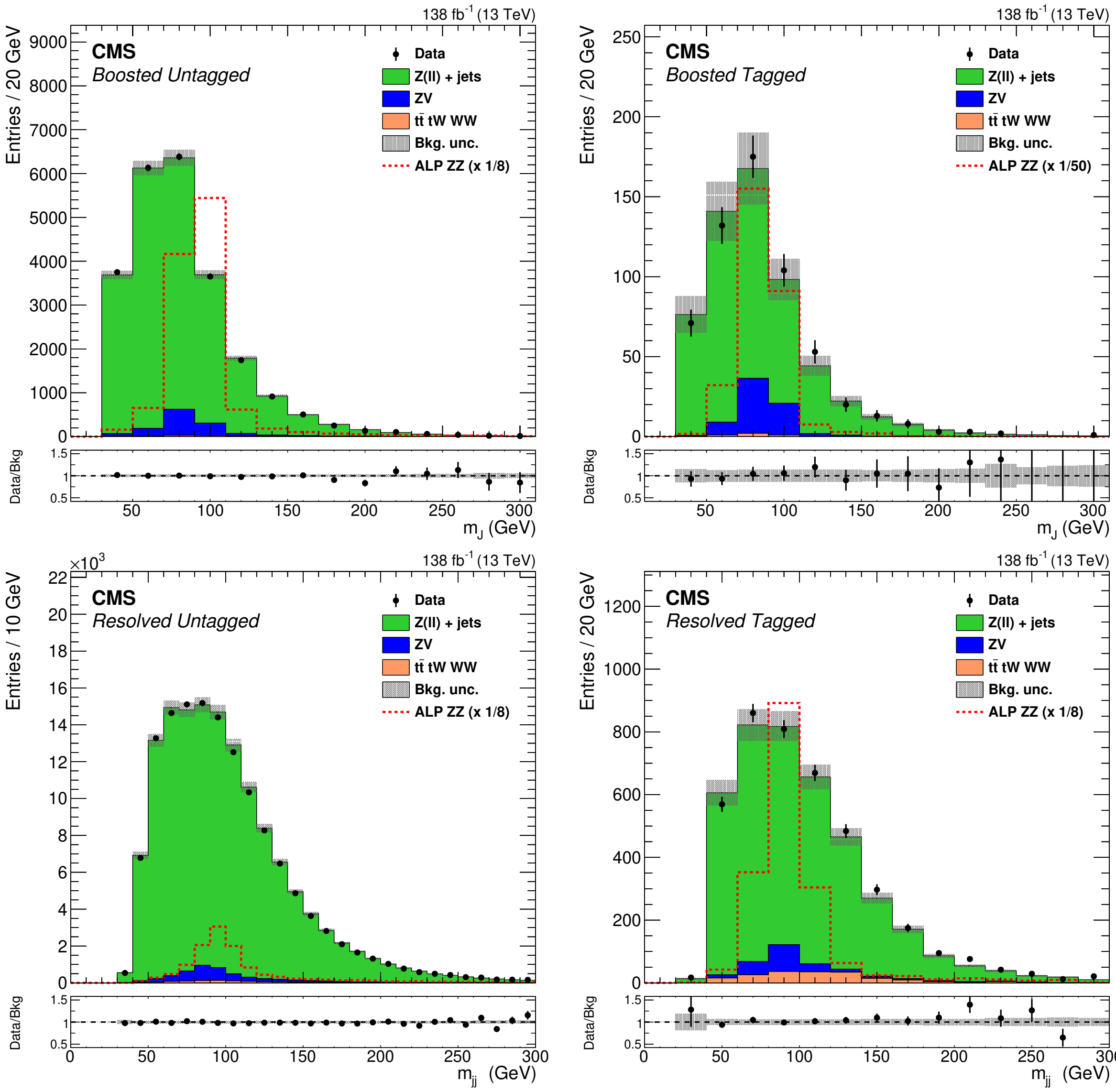

Figure 4: Distributions of the merged jet m_{J} (upper) and the dijet m_{jj} (lower) for the untagged (left) and tagged (right) categories. The distributions include events in the signal regions SR1 and SR2 and in the sideband SB; the corresponding boundaries have been defined in the text. The gray band shows the statistical and systematic uncertainties in the background. Background normalizations are derived from the final fit to the data. The red dashed histograms correspond to a hypothetical linear ALP with 1 TeV^{-1} couplings to gluons and ZZ, and $f_{\mathrm{a}} = 3\,\mathrm{TeV}$; the cross sections have been multiplied by the factors indicated in the legends for better visibility. The lower panels show the ratio of data to background.

6 Background estimation

Most events in the selected ZV and ZH candidate samples come from Z + jets production. A genuine Z boson decaying into $\ell\ell$, along with a high-p_T merged jet or dijet pair, may easily yield a signal-like combination, even though the jets do not originate from a boson decay. The features of the Z + jets background are studied using simulated samples. The limited number of simulated events remaining in the b-tagged categories results in sizable statistical fluctuations in the predicted distributions of the diboson mass m_{ZV} and m_{ZH} for this background. It has been observed, however, that within simulation uncertainties, the shape of the Z + jets mass distribution is the same for events with and without b-tagged jets. Therefore, the Z + jets shapes in the b-tagged categories are described using the m_{ZV} and m_{ZH} shapes obtained from the simulation without making any b tag requirements.

The modeling of the Z + jets background is derived from data. In the final fit to the data, the Z + jets background normalization in the signal region, SR1 or SR2, is constrained by the observed yield in the SB. The shape of the Z + jets mass distribution is determined from the simulation, with a correction applied to improve the agreement with the data in the SB region. A linear function depending on one single parameter s, $\mathrm{corr}(m_{ZX}, s) = 1 + s(m_{ZX} - 500\,\mathrm{GeV})/(500\,\mathrm{GeV})$, is sufficient to make the invariant mass distributions agree within their uncertainties. This procedure is applied independently to each boosted/resolved and untagged/tagged category. Figure 5 shows fits to the SB diboson mass distributions including the linear correction with s at its fitted value. The uncertainties in the SB-fitted slope parameter s are in the range from 0.01 to 0.1, depending on the category. In the final fit of each category, the slope parameter s is allowed to float, constrained by the data in the signal and sideband regions simultaneously. Statistical uncertainties associated with the simulated Z + jets distributions are also taken into account in the fit. The fits in the merged V categories include the peaking region of the background; Fig. 5 shows that the SB data in this particular region are described well by the fit.

Dilepton backgrounds that do not contain a leptonic Z boson decay are estimated from data using eμ events passing the analysis selection. This approach accounts for top quark pair production ($t\bar{t}$), WW + jets, $Z \to \tau\tau$ + jets, single top quark, and hadrons misidentified as leptons; we collectively refer to this set of backgrounds as t + X. The relative normalization and shape of the diboson mass distributions for ee and $\mu\mu$ events with respect to eμ events have been estimated from data on a top quark-enriched control sample and shown to be consistent with lepton flavor symmetry expectations. The t + X background contamination represents 0.8 (0.9)% and 3 (4)% of the total background in the untagged and tagged categories of the resolved SR1 (SR2) selection, while the boosted SR1 (SR2) selection has a contamination of 0.5 (0.7)% and 0.8 (1)% in the untagged and tagged categories.

The diboson background (ZZ and ZW, with $Z \to \ell\ell$) is estimated directly from simulation. The diboson contamination represents 4 (3)% and 8 (4)% of the total background in the untagged and tagged categories of the resolved SR1 (SR2) selection, while the boosted SR1 (SR2) selection has a contamination of about 8 (4)% and 20 (11)% in the untagged and tagged categories. The contribution to the background of SM ZH production, with $Z \to \ell\ell$, has been found to be negligible.

The SR1 m_{ZV} and SR2 m_{ZH} distributions for the boosted and resolved categories are shown in Figs. 6 and 7, respectively.

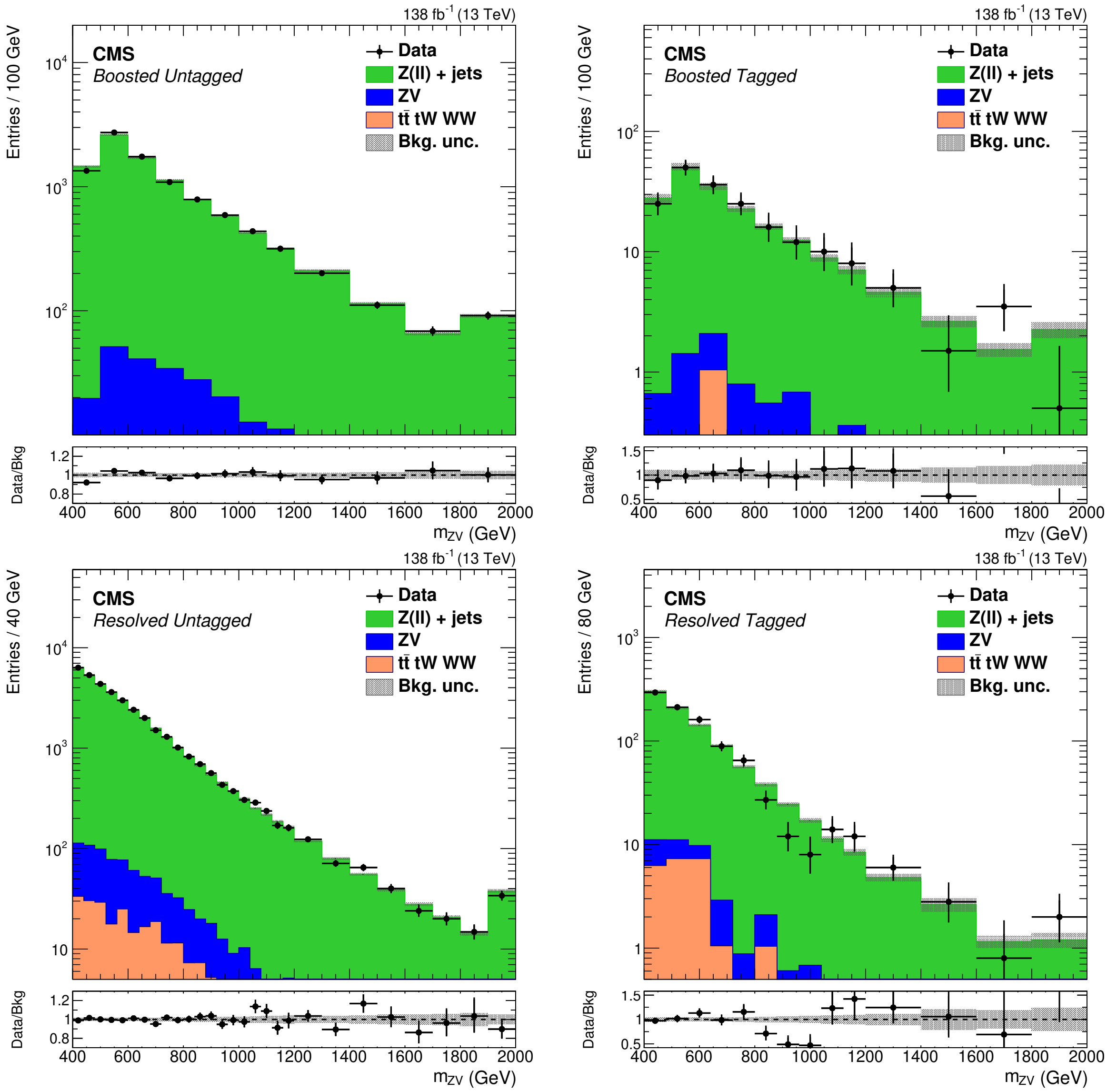

Figure 5: The sideband diboson mass distributions for the boosted V (upper), resolved V (lower), untagged (left), and tagged (right) categories after fitting the sideband data alone. The points show the data, while the filled histograms show the background contributions. The gray band indicates the statistical and post-fit systematic uncertainties in the normalization and shape of the background. The lower panel shows the ratio of data to background.

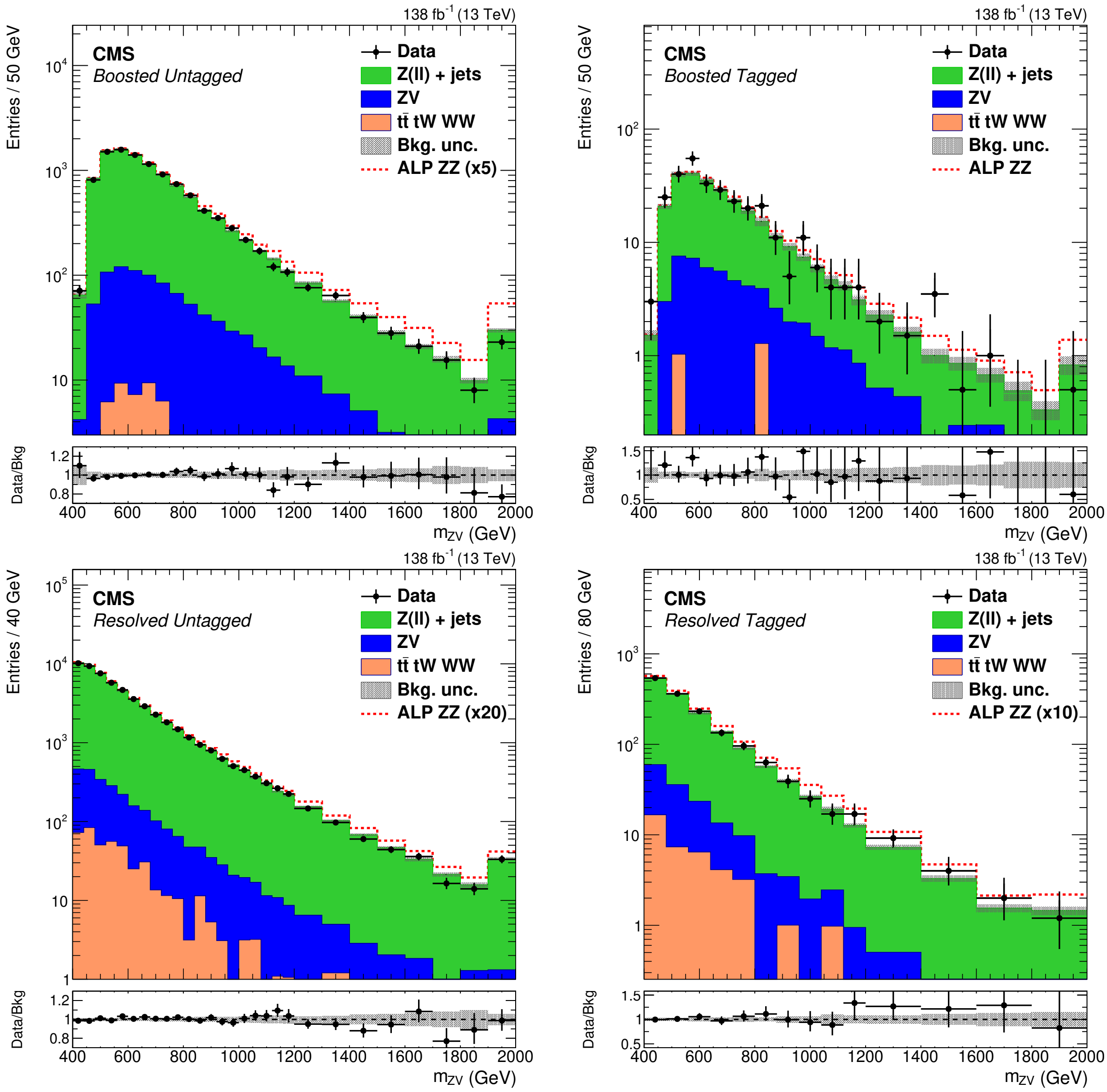

Figure 6: The SR1 m_{ZV} distributions for the boosted V (upper), resolved V (lower), untagged (left), and tagged (right) categories after fitting the signal and sideband regions with a model comprising signal (ALP linear ZZ) plus background. The last bin includes events with m_{ZV} values up to 3000 GeV. The points show the data, while the filled histograms show the background contributions. The signal is represented by the red dashed histogram, normalized to the observed 95% confidence level cross section limit at $f_a = 3$ TeV; the cross sections have been multiplied by the factors indicated in the legends for better visibility. The gray band indicates the statistical and post-fit systematic uncertainties in the normalization and shape of the background. The lower panels show the ratio of data to background.

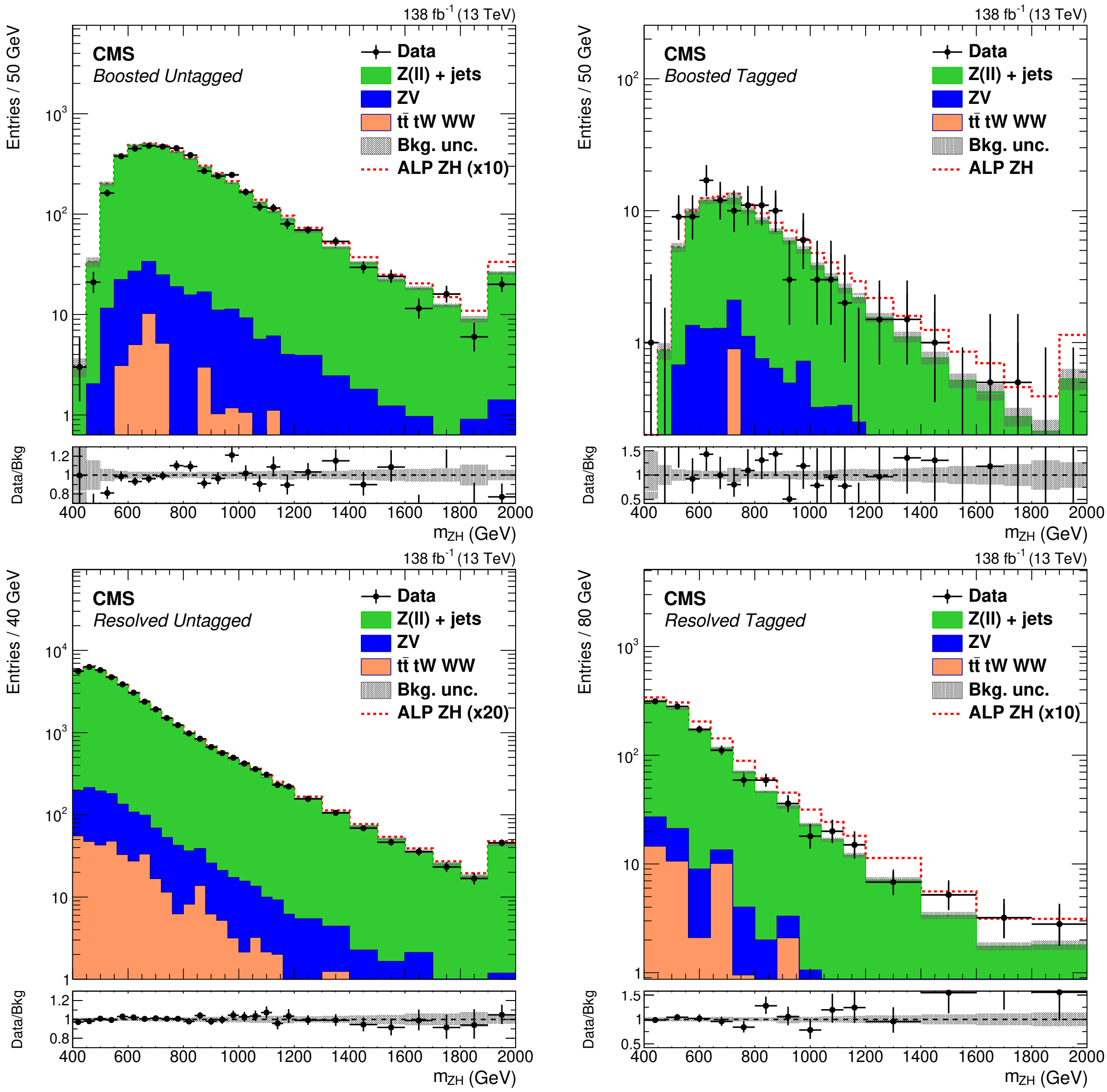

Figure 7: The SR2 m_{ZH} distributions for the boosted H (upper), resolved H (lower), untagged (left), and tagged (right) categories after fitting the signal and sideband regions with a model comprising signal (ALP chiral ZH) plus background. The last bin includes events with m_{ZH} values up to 3000 GeV. The points show the data, while the filled histograms show the background contributions. The signal is represented by the red dashed histogram, normalized to the observed 95% confidence level cross section limit at $f_a = 3$ TeV; the cross sections have been multiplied by the factors indicated in the legends for better visibility. The gray band indicates the statistical and post-fit systematic uncertainties in the normalization and shape of the background. The lower panels show the ratio of data to background.

7 Systematic uncertainties

The systematic uncertainties influence both the normalization and shape of the background and signal distributions in the analysis.

The uncertainty in the background shape, which is the dominant systematic effect, is evaluated by comparing data and simulation after the fit in the signal and SB regions, and the residual shape difference is treated as an uncertainty. The background shape correction procedure has been explained in Section 6. The impacts of these uncertainties are quantified by calculating the change on the fitted signal cross section when a given parameter is displaced by ± 1 standard deviation from its post-fit value, divided by the total uncertainty in the fitted signal cross section. The impacts of the background shape uncertainty in the boosted untagged, boosted tagged, resolved untagged, and resolved tagged categories are 11, 13, 3, and 3%, respectively, for a bulk graviton with a mass of 1 TeV. For an ALP linear ZZ (ALP chiral ZH) signal, the corresponding impacts are 42 (9), 42 (44), 16 (7), and 16 (23)%, respectively.

Uncertainties associated with the description in simulation of the trigger efficiencies, as well as the uncertainties in the efficiency for lepton reconstruction, identification, and isolation, are extracted from dedicated studies of events with leptonic Z boson decays, and amount to 1.5% for muons and 2% for electrons. The uncertainties in the lepton momentum and energy scales are propagated to the signal shape and normalization; the largest impact on the normalization is 0.2%.

Uncertainties in the jet energy scale and resolution [48] affect both the normalization and the shape of the signal samples. The momenta of the reconstructed jets are varied according to the uncertainties in the jet energy scale and resolution, and the selection efficiencies and signal shapes are reevaluated using these modified samples. This procedure results in a change of 1–2% in the normalization of the resolved categories; the largest change in the normalization of the boosted categories is 0.3%. These sources of uncertainty are responsible for the largest signal shape systematic uncertainty.

The uncertainty in the boosted V boson identification efficiency and the groomed mass scale and resolution [54] are responsible for a 7% signal normalization uncertainty in the merged category of the analysis. These are measured in data and simulation in an almost pure selection of semileptonic $\mathrm{t\bar{t}}$ events where boosted W bosons produced in top quark decays are separated from the combinatorial $\mathrm{t\bar{t}}$ background by means of a simultaneous fit to the soft-drop merged-jet mass. The uncertainties in the soft-drop mass scale and resolution are propagated to the groomed jet mass, and the impact on the selection efficiency of signal and ZV background is taken into account. An additional uncertainty affecting the signal normalization is included to account for the extrapolation of the uncertainties extracted from a $\mathrm{t\bar{t}}$ sample at typical jet p_{T} of 200 GeV to higher regimes, yielding an uncertainty of 2.6–6%.

The scale factors (SFs) for the b tagging efficiencies and their corresponding systematic uncertainties are measured in data using samples enriched in b quark content, and their propagation to the signal region of the analysis produces an uncertainty of 12% in the tagged boosted category and 4% in the tagged resolved category. The uncertainties in the mistag efficiency SFs are also considered; the uncertainties in the b tagging and mistag efficiencies are treated as anticorrelated between the tagged and untagged categories.

For the $\mathrm{t} + \mathrm{X}$ background, a 4% uncertainty is estimated by comparing the yield of $\mathrm{e}\mu$ events with $\mathrm{ee} + \mu\mu$ events in a top quark-enriched control region.

The different shapes of the m_{J} (m_{jj}) distributions in the NLO and LO $\mathrm{Z} +$ jets simulations induce a 3 (5)% change in the ratio of the SR to SB normalizations in the boosted (resolved) categories. This difference is taken as a systematic uncertainty.

The effect of varying the factorization and renormalization scales by a factor of 2 is propagated to the signal shape and normalization. The impact on the signal acceptance is evaluated to be 0.1–0.3%, depending on the signal mass and analysis category.

The systematic uncertainty associated with the PDFs used to generate the simulated samples is evaluated by varying the NNPDF 3.0/3.1 PDF set within its uncertainties, following the prescription in Ref. [55], and its effect is propagated to the signal shape and normalization, resulting in a measured uncertainty of 0.3% in the resolved categories and 1.5% in the boosted categories.

Additional systematic uncertainties affecting the normalization of backgrounds and signal from the contributions of pileup events and the integrated luminosity [56–58] are also considered.

The complete list of background and signal normalization systematic uncertainties in the analysis is reported in Table 2.

Table 2: Summary of systematic uncertainties, quoted in percent, affecting the normalization of background and signal samples. Where a systematic uncertainty depends on the signal ZV or ZH channel or mass, the smallest and largest values are reported. In the case of a systematic uncertainty applying only to a specific background source, the source is indicated in parentheses. Systematic uncertainties too small to be considered are written as "<0.1", while a dash (—) represents uncertainties not applicable in the specific analysis category.

	Boosted		Resolved	
Source	Background	Signal	Background	Signal
Integrated luminosity	1.8		1.8	
Electron trigger and ident.	2.0		2.0	
Muon trigger and ident.	1.5		1.5	
Electron energy scale	0.8	<0.1–0.2	0.9	<0.1
Muon momentum scale	0.5	<0.1–0.1	0.6	<0.1
Jet energy scale	1.0	<0.1–0.1	2.8	0.1–1.9
Jet energy resolution	0.3	<0.1–0.3	0.3	1.0
V identification (τ_{21})	5 (ZV)	5	—	—
V identification (extrap.)	—	2.6–6.0	—	—
V mass scale	0.6 (ZV)	0.4–0.8	—	—
V mass resolution	5.0 (ZV)	5.0–6.0	—	—
b tag SF, untagged	0.1	1.0–7.4	0.1	0.7–2.2
b tag SF, tagged	12	12	3.6	4
Mistag SF, untagged	0.3	<0.1–0.2	0.2	0.1
Mistag SF, tagged	3.5	0.1–0.3	3.8	0.4–1.0
SM ZV production	12	—	12	—
t + X normalization	4 (eμ)	—	4 (eμ)	—
SR-to-SB norm. ratio	3 (Z + jets)	—	5 (Z + jets)	—
PDFs	—	1.5–1.6	—	0.3–1.1
Renorm. and fact. scales	—	0.1–0.3	—	0.2–0.3
Pileup	0.5	0.1–0.2	0.1	0.1–0.2

8 Results and interpretation

The signal selection efficiencies obtained from simulation are presented in Table 3.

Table 3: Selection efficiencies in percent for the bulk graviton, W′, and ALP linear and chiral models.

Analysis	500 GeV	600 GeV	800 GeV	1000 GeV	1200 GeV	1400 GeV	1600 GeV	1800 GeV
Bulk graviton								
Boosted	8	22	33	37	38	38	37	36
Resolved	21	15	12	9	6	4	3	2
Combined	29	37	44	46	44	42	40	38
W′								
Boosted	12	25	35	39	40	39	39	37
Resolved	14	10	9	6	4	3	2	1
Combined	26	35	43	45	44	42	40	38
	ALP linear ZZ				ALP chiral ZH			
Boosted	8				7			
Resolved	7				10			
Combined	15				17			

Results are extracted from a combined maximum likelihood fit of signal and background to the m_{ZV} or m_{ZH} distribution in the 400–3000 GeV interval, simultaneously in all the categories used in the analysis. The systematic uncertainties discussed in Section 7 are included as nuisance parameters in the maximum likelihood fit, and the background-only hypothesis is tested against the combined background and signal hypothesis [59, 60].

No significant excess is observed with respect to the SM expectations. Upper limits at 95% confidence level (CL) on the signal production cross sections are set using the modified frequentist (CL_s) approach in the asymptotic approximation [59–62].

The observed and expected upper limits on the resonance cross section, multiplied by the branching fraction for the decay into one Z boson and a W or Z boson, $\sigma_G \mathcal{B}(G \to ZZ)$ or $\sigma_{W'} \mathcal{B}(W' \to ZW)$, are reported as a function of the resonance mass in Fig. 8, assuming a W′ or G produced in the narrow-width approximation. A WED bulk graviton is excluded up to masses of 1200 (expected 1150) GeV for $\widetilde{\kappa} = 0.5$. These limits improve on those previously obtained by the CMS Collaboration in the analogous final states [12]. The current W′ mass exclusion limits in HVT models A ($g_V = 1$) and B ($g_V = 3$) are those derived from the high-mass analysis in Ref. [12].

Figure 9 shows the observed and expected 95% CL upper limits on the ALP linear $|c_{\widetilde{G}} c_{\widetilde{Z}}|$ (left) and the ALP chiral $|c_{\widetilde{G}} \widetilde{a}_{2D}|$ (right) coupling coefficients, as functions of the mass scale f_a. For each black dot in Fig. 9, events with m_{ZV} or $m_{ZH} > f_a$ have been excluded from the fit, restricting the analysis to the EFT mass consistency region. Limits on the coupling coefficients for $f_a > 3$ TeV are calculated from the same fit result as $f_a = 3$ TeV. We define the ALP mass range where our results are considered valid as the region where the cross section diverges by less than 10% from its asymptotic value, $m_a < 100$ GeV. The expected and observed upper limits on $\sigma(gg \to a^* \to ZZ/ZH)$ for $f_a = 3$ TeV are reported in Table 4.

In the ALP linear model with $f_a \geq 3$ TeV, the observed (expected) 95% CL limit on $|c_{\widetilde{G}} c_{\widetilde{Z}}|/f_a^2$ is 0.0415 (0.0400) TeV $^{-2}$. The limit on $|c_{\widetilde{Z}}|/f_a$ and $|c_{\widetilde{G}}|/f_a$ in the case where the two are equal is 0.204 (0.200) TeV $^{-1}$; for $|c_{\widetilde{G}}|/f_a = 0.25\,\text{TeV}^{-1}$, the limit on $|c_{\widetilde{Z}}|/f_a$ is 0.166 (0.160) TeV $^{-1}$.

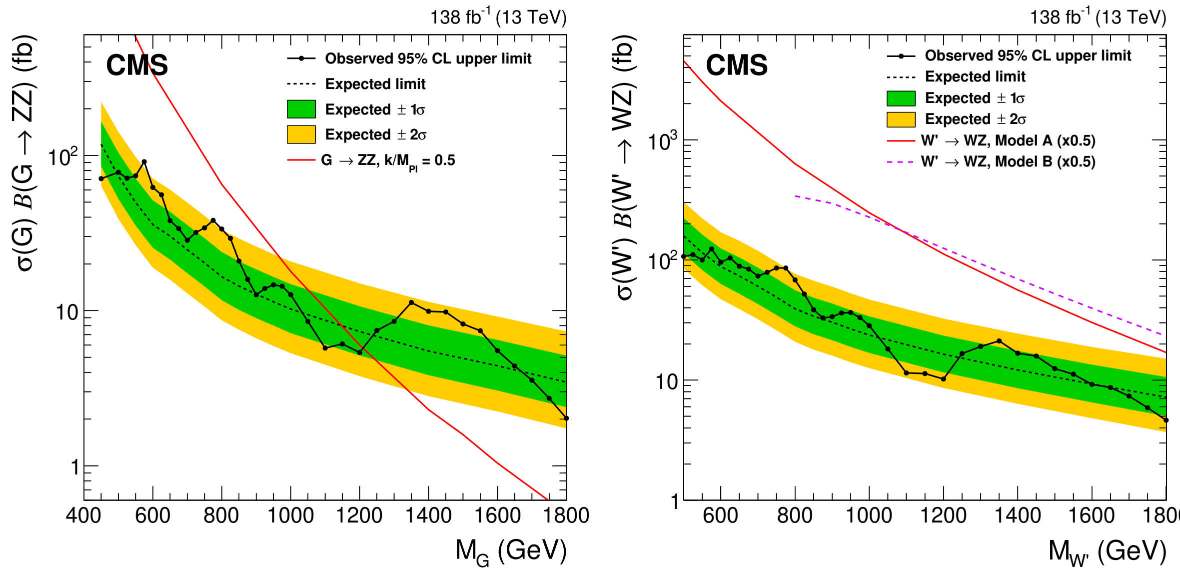

Figure 8: Observed and expected 95% CL upper limits on $\sigma_{\mathrm{G}}\,\mathcal{B}(\mathrm{G} \to \mathrm{ZZ})$ (left) and $\sigma_{\mathrm{W}'}\,\mathcal{B}(\mathrm{W}' \to \mathrm{ZW})$ (right) as a function of the resonance mass, taking into account all statistical and systematic uncertainties. The electron and muon channels and the various categories used in the analysis are combined together. The green (inner) and yellow (outer) bands represent the 68 and 95% coverage of the expected limit in the background-only hypothesis. Theoretical predictions for the signal production cross section are also shown: (left) G produced in the WED bulk graviton model with $\tilde{\kappa} = 0.5$; (right) W' produced in the framework of HVT model A and B with $g_{\mathrm{V}} = 1$ and 3, respectively.

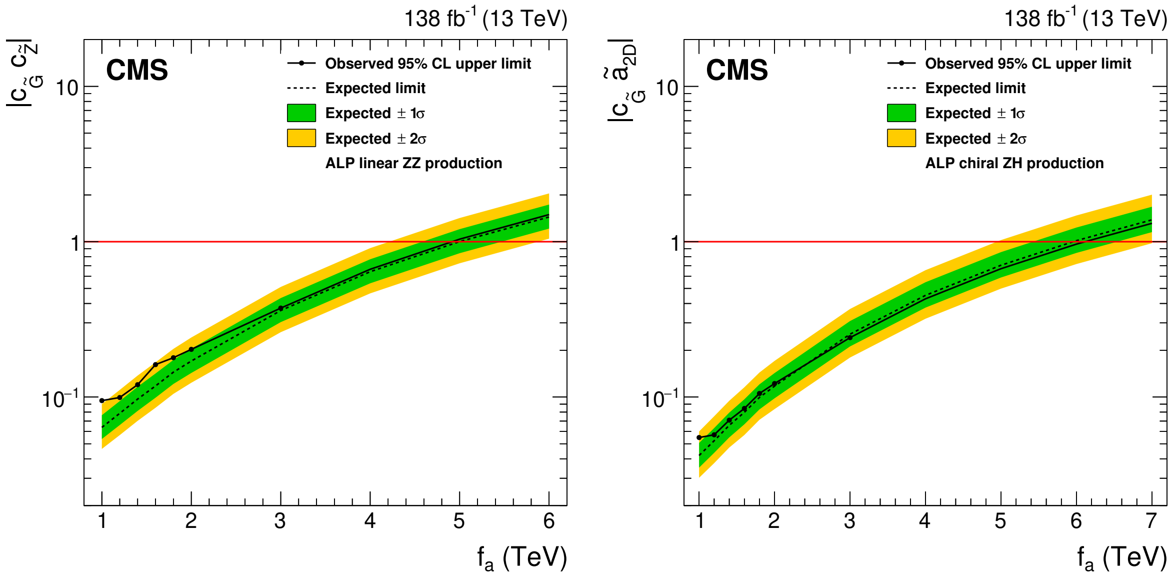

Figure 9: Observed and expected 95% CL upper limits on the ALP linear $|c_{\widetilde{\mathrm{G}}}c_{\widetilde{\mathrm{Z}}}|$ (left) and the ALP chiral $|c_{\widetilde{\mathrm{G}}}\widetilde{a}_{2\mathrm{D}}|$ (right) coupling coefficients as a function of the mass scale f_{a} for ALP masses $m_{\mathrm{a}} < 100\,\mathrm{GeV}$.

Table 4: Expected and observed 95% CL upper limits on $\sigma(\mathrm{gg} \rightarrow \mathrm{a}^* \rightarrow \mathrm{ZZ/ZH})$ in fb for $f_\mathrm{a} = 3\,\mathrm{TeV}$. The $\pm 1\sigma$ and $\pm 2\sigma$ numbers represent the 68 and 95% coverage of the expected limit for the background-only hypothesis.

Model	Expected -2σ	Expected -1σ	Expected Median	Expected $+1\sigma$	Expected $+2\sigma$	Observed
ALP linear ZZ	79	107	151	218	304	162
ALP chiral ZH	32	39	64	94	134	57

In the ALP chiral model with $f_\mathrm{a} \geq 3\,\mathrm{TeV}$, the observed (expected) 95% CL limit on $|c_{\widetilde{\mathrm{G}}} \widetilde{a}_{2\mathrm{D}}|/f_\mathrm{a}^2$ is 0.0269 (0.0281) TeV $^{-2}$. The limit on $|\widetilde{a}_{2\mathrm{D}}|/f_\mathrm{a}$ and $|c_{\widetilde{\mathrm{G}}}|/f_\mathrm{a}$ in the case where the two are equal is 0.164 (0.168) TeV $^{-1}$; for $|c_{\widetilde{\mathrm{G}}}|/f_\mathrm{a} = 0.25\,\mathrm{TeV}^{-1}$, the limit on $|\widetilde{a}_{2\mathrm{D}}|/f_\mathrm{a}$ is 0.108 (0.113) TeV $^{-1}$. These limits are valid for a Higgs boson with SM decays. The experimental upper limit on $\mathcal{B}(\mathrm{H} \rightarrow \mathrm{BSM})$ is 0.34 at 95% CL [63]; thus, relaxing the SM condition would increase the limits on $|c_{\widetilde{\mathrm{G}}} \widetilde{a}_{2\mathrm{D}}|/f_\mathrm{a}^2$ by a factor of 1.23 at most.

9 Summary

A search has been presented for heavy resonances decaying to ZZ or ZW, and nonresonant ZZ or ZH production (where H is the Higgs boson) mediated by axion-like particles (ALPs). The analysis is sensitive to resonances with masses in the range from 450 to 1800 GeV. Two categories are defined based on the merged or resolved reconstruction of the hadronically decaying boson. The search is based on data collected in 2016–2018 by the CMS experiment at the LHC in proton-proton collisions with a center-of-mass energy of 13 TeV, corresponding to an integrated luminosity of 138 fb^{-1}.

No significant excess is observed in the data above the standard model expectations. Depending on the resonance mass, upper limits of 2–90 and 5–120 fb have been set on the product of the cross section of a spin-2 bulk graviton and the ZZ branching fraction, and on a spin-1 W' signal and the ZW branching fraction, respectively. Upper limits on the nonresonant ALP-mediated ZZ and ZH production cross sections for a new physics energy scale $f_\mathrm{a} = 3\,\mathrm{TeV}$ and ALP masses $m_\mathrm{a} < 100\,\mathrm{GeV}$ have been established at 162 and 57 fb, respectively. Depending on the value of the scale f_a, upper limits on the product of the ALP coupling to gluons with the relevant coupling to ZZ or ZH of 0.02–0.09 TeV $^{-2}$ have been set, valid for ALP masses $m_\mathrm{a} < 100\,\mathrm{GeV}$. These are the first limits based on nonresonant ALP-mediated ZZ and ZH production obtained by the LHC experiments.

Acknowledgments

We congratulate our colleagues in the CERN accelerator departments for the excellent performance of the LHC and thank the technical and administrative staffs at CERN and at other CMS institutes for their contributions to the success of the CMS effort. In addition, we gratefully acknowledge the computing centers and personnel of the Worldwide LHC Computing Grid and other centers for delivering so effectively the computing infrastructure essential to our analyses. Finally, we acknowledge the enduring support for the construction and operation of the LHC, the CMS detector, and the supporting computing infrastructure provided by the following funding agencies: BMBWF and FWF (Austria); FNRS and FWO (Belgium); CNPq, CAPES, FAPERJ, FAPERGS, and FAPESP (Brazil); MES and BNSF (Bulgaria); CERN; CAS, MoST, and NSFC (China); MINCIENCIAS (Colombia); MSES and CSF (Croatia); RIF (Cyprus); SENESCYT

(Ecuador); MoER, ERC PUT and ERDF (Estonia); Academy of Finland, MEC, and HIP (Finland); CEA and CNRS/IN2P3 (France); BMBF, DFG, and HGF (Germany); GSRI (Greece); NKFIA (Hungary); DAE and DST (India); IPM (Iran); SFI (Ireland); INFN (Italy); MSIP and NRF (Republic of Korea); MES (Latvia); LAS (Lithuania); MOE and UM (Malaysia); BUAP, CINVESTAV, CONACYT, LNS, SEP, and UASLP-FAI (Mexico); MOS (Montenegro); MBIE (New Zealand); PAEC (Pakistan); MSHE and NSC (Poland); FCT (Portugal); JINR (Dubna); MON, RosAtom, RAS, RFBR, and NRC KI (Russia); MESTD (Serbia); SEIDI, CPAN, PCTI, and FEDER (Spain); MOSTR (Sri Lanka); Swiss Funding Agencies (Switzerland); MST (Taipei); ThEPCenter, IPST, STAR, and NSTDA (Thailand); TUBITAK and TAEK (Turkey); NASU (Ukraine); STFC (United Kingdom); DOE and NSF (USA).

Individuals have received support from the Marie-Curie program and the European Research Council and Horizon 2020 Grant, contract Nos. 675440, 724704, 752730, 758316, 765710, 824093, 884104, and COST Action CA16108 (European Union); the Leventis Foundation; the Alfred P. Sloan Foundation; the Alexander von Humboldt Foundation; the Belgian Federal Science Policy Office; the Fonds pour la Formation à la Recherche dans l'Industrie et dans l'Agriculture (FRIA-Belgium); the Agentschap voor Innovatie door Wetenschap en Technologie (IWT-Belgium); the F.R.S.-FNRS and FWO (Belgium) under the "Excellence of Science – EOS" – be.h project n. 30820817; the Beijing Municipal Science & Technology Commission, No. Z191100007219010; the Ministry of Education, Youth and Sports (MEYS) of the Czech Republic; the Deutsche Forschungsgemeinschaft (DFG), under Germany's Excellence Strategy – EXC 2121 "Quantum Universe" – 390833306, and under project number 400140256 - GRK2497; the Lendület ("Momentum") Program and the János Bolyai Research Scholarship of the Hungarian Academy of Sciences, the New National Excellence Program ÚNKP, the NKFIA research grants 123842, 123959, 124845, 124850, 125105, 128713, 128786, and 129058 (Hungary); the Council of Science and Industrial Research, India; the Latvian Council of Science; the Ministry of Science and Higher Education and the National Science Center, contracts Opus 2014/15/B/ST2/03998 and 2015/19/B/ST2/02861 (Poland); the Fundação para a Ciência e a Tecnologia, grant CEECIND/01334/2018 (Portugal); the National Priorities Research Program by Qatar National Research Fund; the Ministry of Science and Higher Education, projects no. 14.W03.31.0026 and no. FSWW-2020-0008, and the Russian Foundation for Basic Research, project No.19-42-703014 (Russia); the Programa Estatal de Fomento de la Investigación Científica y Técnica de Excelencia María de Maeztu, grant MDM-2015-0509 and the Programa Severo Ochoa del Principado de Asturias; the Stavros Niarchos Foundation (Greece); the Rachadapisek Sompot Fund for Postdoctoral Fellowship, Chulalongkorn University and the Chulalongkorn Academic into Its 2nd Century Project Advancement Project (Thailand); the Kavli Foundation; the Nvidia Corporation; the SuperMicro Corporation; the Welch Foundation, contract C-1845; and the Weston Havens Foundation (USA).

References

[1] K. Agashe, H. Davoudiasl, G. Perez, and A. Soni, "Warped gravitons at the LHC and beyond", *Phys. Rev. D* **76** (2007) 036006, doi:10.1103/PhysRevD.76.036006, arXiv:hep-ph/0701186.

[2] L. Randall and R. Sundrum, "A large mass hierarchy from a small extra dimension", *Phys. Rev. Lett.* **83** (1999) 3370, doi:10.1103/PhysRevLett.83.3370, arXiv:hep-ph/9905221.

[3] L. Randall and R. Sundrum, "An alternative to compactification", *Phys. Rev. Lett.* **83** (1999) 4690, doi:10.1103/PhysRevLett.83.4690, arXiv:hep-th/9906064.

[4] D. Pappadopulo, A. Thamm, R. Torre, and A. Wulzer, "Heavy vector triplets: Bridging theory and data", *JHEP* **09** (2014) 060, doi:10.1007/JHEP09(2014)060, arXiv:1402.4431.

[5] H. Georgi, D. B. Kaplan, and L. Randall, "Manifesting the invisible axion at low energies", *Phys. Lett. B* **169** (1986) 73, doi:10.1016/0370-2693(86)90688-X.

[6] K. Choi, K. Kang, and J. E. Kim, "Effects of η' in low-energy axion physics", *Phys. Lett. B* **181** (1986) 145, doi:10.1016/0370-2693(86)91273-6.

[7] I. Brivio et al., "ALPs effective field theory and collider signatures", *Eur. Phys. J. C* **77** (2017) 572, doi:10.1140/epjc/s10052-017-5111-3, arXiv:1701.05379.

[8] M. Bauer, M. Neubert, and A. Thamm, "Collider probes of axion-like particles", *JHEP* **12** (2017) 044, doi:10.1007/JHEP12(2017)044, arXiv:1708.00443.

[9] M. B. Gavela, J. M. No, V. Sanz, and J. F. de Trocóniz, "Nonresonant searches for axionlike particles at the LHC", *Phys. Rev. Lett.* **124** (2020) 051802, doi:10.1103/PhysRevLett.124.051802, arXiv:1905.12953.

[10] CMS Collaboration, "Jet energy scale and resolution in the CMS experiment in pp collisions at 8 TeV", *JINST* **12** (2017) P02014, doi:10.1088/1748-0221/12/02/P02014, arXiv:1607.03663.

[11] CMS Collaboration, "Search for a heavy resonance decaying into a Z boson and a vector boson in the $\nu\overline{\nu}\mathrm{q}\overline{\mathrm{q}}$ final state", *JHEP* **07** (2018) 075, doi:10.1007/JHEP07(2018)075, arXiv:1803.03838.

[12] CMS Collaboration, "Search for a heavy resonance decaying into a Z boson and a Z or W boson in $2\ell 2\mathrm{q}$ final states at $\sqrt{s} = 13$ TeV", *JHEP* **09** (2018) 101, doi:10.1007/JHEP09(2018)101, arXiv:1803.10093.

[13] CMS Collaboration, "Combination of CMS searches for heavy resonances decaying to pairs of bosons or leptons", *Phys. Lett. B* **798** (2019) 134952, doi:10.1016/j.physletb.2019.134952, arXiv:1906.00057.

[14] ATLAS Collaboration, "Search for heavy diboson resonances in semileptonic final states in pp collisions at $\sqrt{s} = 13$ TeV with the ATLAS detector", *Eur. Phys. J. C* **80** (2020) 1165, doi:10.1140/epjc/s10052-020-08554-y, arXiv:2004.14636.

[15] CMS Collaboration, "Search for a heavy vector resonance decaying to a Z boson and a Higgs boson in proton-proton collisions at $\sqrt{s} = 13$ TeV", *Eur. Phys. J. C* **81** (2021) 688, doi:10.1140/epjc/s10052-021-09348-6, arXiv:2102.08198.

[16] S. Carra et al., "Constraining off-shell production of axion-like particles with $Z\gamma$ and WW differential cross-section measurements", 2021. arXiv:2106.10085.

[17] "HEPData record for this analysis", 2021. doi:10.17182/hepdata.114367.

[18] A. L. Fitzpatrick, J. Kaplan, L. Randall, and L.-T. Wang, "Searching for the Kaluza-Klein graviton in bulk RS models", *JHEP* **09** (2007) 013, doi:10.1088/1126-6708/2007/09/013, arXiv:hep-ph/0701150.

[19] W. D. Goldberger and M. B. Wise, “Modulus stabilization with bulk fields”, *Phys. Rev. Lett.* **83** (1999) 4922, doi:10.1103/PhysRevLett.83.4922, arXiv:hep-ph/9907447.

[20] A. Carvalho, “Gravity particles from warped extra dimensions, predictions for LHC”, 2014. arXiv:1404.0102.

[21] J. Alwall et al., “The automated computation of tree-level and next-to-leading order differential cross sections, and their matching to parton shower simulations”, *JHEP* **07** (2014) 079, doi:10.1007/JHEP07(2014)079, arXiv:1405.0301.

[22] W. Buchmuller and D. Wyler, “Effective Lagrangian analysis of new interactions and flavor conservation”, *Nucl. Phys. B* **268** (1986) 621, doi:10.1016/0550-3213(86)90262-2.

[23] B. Grzadkowski, M. Iskrzynski, M. Misiak, and J. Rosiek, “Dimension-six terms in the standard model Lagrangian”, *JHEP* **10** (2010) 085, doi:10.1007/JHEP10(2010)085, arXiv:1008.4884.

[24] F. Feruglio, “The chiral approach to the electroweak interactions”, *Int. J. Mod. Phys. A* **8** (1993) 4937, doi:10.1142/S0217751X93001946, arXiv:hep-ph/9301281.

[25] A. Azatov, R. Contino, and J. Galloway, “Model-independent bounds on a light Higgs”, *JHEP* **04** (2012) 127, doi:10.1007/JHEP04(2012)127, arXiv:1202.3415. [Erratum: doi:10.1007/JHEP04(2013)140].

[26] R. Alonso et al., “The effective chiral Lagrangian for a light dynamical Higgs particle”, *Phys. Lett. B* **722** (2013) 330, doi:10.1016/j.physletb.2013.04.037, arXiv:1212.3305. [Erratum: doi:10.1016/j.physletb.2013.09.028].

[27] G. Buchalla, O. Catà, and C. Krause, “Complete electroweak chiral Lagrangian with a light Higgs at NLO”, *Nucl. Phys. B* **880** (2014) 552, doi:10.1016/j.nuclphysb.2014.01.018, arXiv:1307.5017. [Erratum: doi:10.1016/j.nuclphysb.2016.09.010].

[28] J. M. Lindert et al., “Precise predictions for $V+$ jets dark matter backgrounds”, *Eur. Phys. J. C* **77** (2017) 829, doi:10.1140/epjc/s10052-017-5389-1, arXiv:1705.04664.

[29] T. Sjöstrand et al., “An introduction to PYTHIA 8.2”, *Comput. Phys. Commun.* **191** (2015) 159, doi:10.1016/j.cpc.2015.01.024, arXiv:1410.3012.

[30] CMS Collaboration, “Event generator tunes obtained from underlying event and multiparton scattering measurements”, *Eur. Phys. J. C* **76** (2016) 155, doi:10.1140/epjc/s10052-016-3988-x, arXiv:1512.00815.

[31] CMS Collaboration, “Extraction and validation of a new set of CMS PYTHIA8 tunes from underlying-event measurements”, *Eur. Phys. J. C* **80** (2020) 4, doi:10.1140/epjc/s10052-019-7499-4, arXiv:1903.12179.

[32] NNPDF Collaboration, “Parton distributions for the LHC Run II”, *JHEP* **04** (2015) 040, doi:10.1007/JHEP04(2015)040, arXiv:1410.8849.

[33] NNPDF Collaboration, “Parton distributions from high-precision collider data”, *Eur. Phys. J. C* **77** (2017) 663, doi:10.1140/epjc/s10052-017-5199-5, arXiv:1706.00428.

[34] GEANT4 Collaboration, "GEANT4—a simulation toolkit", *Nucl. Instrum. Meth. A* **506** (2003) 250, doi:10.1016/S0168-9002(03)01368-8.

[35] CMS Collaboration, "Performance of the CMS level-1 trigger in proton-proton collisions at $\sqrt{s} = 13\,\text{TeV}$", *JINST* **15** (2020) P10017, doi:10.1088/1748-0221/15/10/P10017, arXiv:2006.10165.

[36] CMS Collaboration, "The CMS trigger system", *JINST* **12** (2017) P01020, doi:10.1088/1748-0221/12/01/P01020, arXiv:1609.02366.

[37] CMS Collaboration, "The CMS experiment at the CERN LHC", *JINST* **3** (2008) S08004, doi:10.1088/1748-0221/3/08/S08004.

[38] CMS Collaboration, "Particle-flow reconstruction and global event description with the CMS detector", *JINST* **12** (2017) P10003, doi:10.1088/1748-0221/12/10/P10003, arXiv:1706.04965.

[39] M. Cacciari, G. P. Salam, and G. Soyez, "The anti-k_{T} jet clustering algorithm", *JHEP* **04** (2008) 063, doi:10.1088/1126-6708/2008/04/063, arXiv:0802.1189.

[40] M. Cacciari, G. P. Salam, and G. Soyez, "FastJet user manual", *Eur. Phys. J. C* **72** (2012) 1896, doi:10.1140/epjc/s10052-012-1896-2, arXiv:1111.6097.

[41] CMS Collaboration, "Description and performance of track and primary-vertex reconstruction with the CMS tracker", *JINST* **9** (2014) P10009, doi:10.1088/1748-0221/9/10/P10009, arXiv:1405.6569.

[42] CMS Tracker Group Collaboration, "The CMS phase-1 pixel detector upgrade", *JINST* **16** (2021) P02027, doi:10.1088/1748-0221/16/02/P02027, arXiv:2012.14304.

[43] CMS Collaboration, "Track impact parameter resolution for the full pseudo rapidity coverage in the 2017 dataset with the CMS phase-1 pixel detector", CMS Detector Performance Summary CMS-DP-2020-049, 2020.

[44] CMS Collaboration, "Performance of electron reconstruction and selection with the CMS detector in proton-proton collisions at $\sqrt{s} = 8\,\text{TeV}$", *JINST* **10** (2015) P06005, doi:10.1088/1748-0221/10/06/P06005, arXiv:1502.02701.

[45] CMS Collaboration, "Performance of the CMS muon detector and muon reconstruction with proton-proton collisions at $\sqrt{s} = 13\,\text{TeV}$", *JINST* **13** (2018) P06015, doi:10.1088/1748-0221/13/06/P06015, arXiv:1804.04528.

[46] CMS Collaboration, "Pileup mitigation at CMS in 13 TeV data", *JINST* **15** (2020) P09018, doi:10.1088/1748-0221/15/09/p09018, arXiv:2003.00503.

[47] D. Bertolini, P. Harris, M. Low, and N. Tran, "Pileup per particle identification", *JHEP* **10** (2014) 059, doi:10.1007/JHEP10(2014)059, arXiv:1407.6013.

[48] CMS Collaboration, "Jet algorithms performance in 13 TeV data", CMS Physics Analysis Summary CMS-PAS-JME-16-003, 2017.

[49] M. Dasgupta, A. Fregoso, S. Marzani, and G. P. Salam, "Towards an understanding of jet substructure", *JHEP* **09** (2013) 029, doi:10.1007/JHEP09(2013)029, arXiv:1307.0007.

[50] A. J. Larkoski, S. Marzani, G. Soyez, and J. Thaler, "Soft drop", *JHEP* **05** (2014) 146, doi:10.1007/JHEP05(2014)146, arXiv:1402.2657.

[51] J. Thaler and K. Van Tilburg, "Identifying boosted objects with N-subjettiness", *JHEP* **03** (2011) 015, doi:10.1007/JHEP03(2011)015, arXiv:1011.2268.

[52] CMS Collaboration, "Identification of heavy-flavour jets with the CMS detector in pp collisions at 13 TeV", *JINST* **13** (2018) P05011, doi:10.1088/1748-0221/13/05/P05011, arXiv:1712.07158.

[53] CMS Collaboration, "Measurement of the inclusive W and Z production cross sections in pp collisions at $\sqrt{s} = 7$ TeV", *JHEP* **10** (2011) 132, doi:10.1007/JHEP10(2011)132, arXiv:1107.4789.

[54] CMS Collaboration, "Identification techniques for highly boosted W bosons that decay into hadrons", *JHEP* **12** (2014) 017, doi:10.1007/JHEP12(2014)017, arXiv:1410.4227.

[55] J. Butterworth et al., "PDF4LHC recommendations for LHC Run II", *J. Phys. G* **43** (2016) 023001, doi:10.1088/0954-3899/43/2/023001, arXiv:1510.03865.

[56] CMS Collaboration, "Precision luminosity measurement in proton-proton collisions at $\sqrt{s} = 13$ TeV in 2015 and 2016 at CMS", *Eur. Phys. J. C* **81** (2021) 800, doi:10.1140/epjc/s10052-021-09538-2, arXiv:2104.01927.

[57] CMS Collaboration, "CMS luminosity measurement for the 2017 data-taking period at $\sqrt{s}$ = 13 TeV", CMS Physics Analysis Summary CMS-PAS-LUM-17-004, 2018.

[58] CMS Collaboration, "CMS luminosity measurement for the 2018 data-taking period at $\sqrt{s} = 13$ TeV", CMS Physics Analysis Summary CMS-PAS-LUM-18-002, 2019.

[59] A. L. Read, "Presentation of search results: The CL_s technique", *J. Phys. G* **28** (2002) 2693, doi:10.1088/0954-3899/28/10/313.

[60] T. Junk, "Confidence level computation for combining searches with small statistics", *Nucl. Instrum. Meth. A* **434** (1999) 435, doi:10.1016/S0168-9002(99)00498-2, arXiv:hep-ex/9902006.

[61] G. Cowan, K. Cranmer, E. Gross, and O. Vitells, "Asymptotic formulae for likelihood-based tests of new physics", *Eur. Phys. J. C* **71** (2011) 1554, doi:10.1140/epjc/s10052-011-1554-0, arXiv:1007.1727. [Erratum: doi:10.1140/epjc/s10052-013-2501-z].

[62] ATLAS Collaboration, CMS Collaboration, LHC Higgs Combination Group, "Procedure for the LHC Higgs boson search combination in Summer 2011", Technical Report CMS-NOTE-2011-005, ATL-PHYS-PUB-2011-11, 2011.

[63] ATLAS and CMS Collaborations, "Measurements of the Higgs boson production and decay rates and constraints on its couplings from a combined ATLAS and CMS analysis of the LHC pp collision data at $\sqrt{s} = 7$ and 8 TeV", *JHEP* **08** (2016) 045, doi:10.1007/JHEP08(2016)045, arXiv:1606.02266.

A The CMS Collaboration

Yerevan Physics Institute, Yerevan, Armenia
A. Tumasyan

Institut für Hochenergiephysik, Vienna, Austria
W. Adam, J.W. Andrejkovic, T. Bergauer, S. Chatterjee, K. Damanakis, M. Dragicevic, A. Escalante Del Valle, R. Frühwirth[1], M. Jeitler[1], N. Krammer, L. Lechner, D. Liko, I. Mikulec, P. Paulitsch, F.M. Pitters, J. Schieck[1], R. Schöfbeck, D. Schwarz, S. Templ, W. Waltenberger, C.-E. Wulz[1]

Institute for Nuclear Problems, Minsk, Belarus
V. Chekhovsky, A. Litomin, V. Makarenko

Universiteit Antwerpen, Antwerpen, Belgium
M.R. Darwish[2], E.A. De Wolf, T. Janssen, T. Kello[3], A. Lelek, H. Rejeb Sfar, P. Van Mechelen, S. Van Putte, N. Van Remortel

Vrije Universiteit Brussel, Brussel, Belgium
F. Blekman, E.S. Bols, J. D'Hondt, M. Delcourt, H. El Faham, S. Lowette, S. Moortgat, A. Morton, D. Müller, A.R. Sahasransu, S. Tavernier, W. Van Doninck

Université Libre de Bruxelles, Bruxelles, Belgium
D. Beghin, B. Bilin, B. Clerbaux, G. De Lentdecker, L. Favart, A. Grebenyuk, A.K. Kalsi, K. Lee, M. Mahdavikhorrami, I. Makarenko, L. Moureaux, L. Pétré, A. Popov, N. Postiau, E. Starling, L. Thomas, M. Vanden Bemden, C. Vander Velde, P. Vanlaer

Ghent University, Ghent, Belgium
T. Cornelis, D. Dobur, J. Knolle, L. Lambrecht, G. Mestdach, M. Niedziela, C. Roskas, A. Samalan, K. Skovpen, M. Tytgat, B. Vermassen, L. Wezenbeek

Université Catholique de Louvain, Louvain-la-Neuve, Belgium
A. Benecke, A. Bethani, G. Bruno, F. Bury, C. Caputo, P. David, C. Delaere, I.S. Donertas, A. Giammanco, K. Jaffel, Sa. Jain, V. Lemaitre, K. Mondal, J. Prisciandaro, A. Taliercio, M. Teklishyn, T.T. Tran, P. Vischia, S. Wertz

Centro Brasileiro de Pesquisas Fisicas, Rio de Janeiro, Brazil
G.A. Alves, C. Hensel, A. Moraes

Universidade do Estado do Rio de Janeiro, Rio de Janeiro, Brazil
W.L. Aldá Júnior, M. Alves Gallo Pereira, M. Barroso Ferreira Filho, H. Brandao Malbouisson, W. Carvalho, J. Chinellato[4], E.M. Da Costa, G.G. Da Silveira[5], D. De Jesus Damiao, S. Fonseca De Souza, C. Mora Herrera, K. Mota Amarilo, L. Mundim, H. Nogima, P. Rebello Teles, A. Santoro, S.M. Silva Do Amaral, A. Sznajder, M. Thiel, F. Torres Da Silva De Araujo[6], A. Vilela Pereira

Universidade Estadual Paulista (a), Universidade Federal do ABC (b), São Paulo, Brazil
C.A. Bernardes[5], L. Calligaris, T.R. Fernandez Perez Tomei, E.M. Gregores, D.S. Lemos, P.G. Mercadante, S.F. Novaes, Sandra S. Padula

Institute for Nuclear Research and Nuclear Energy, Bulgarian Academy of Sciences, Sofia, Bulgaria
A. Aleksandrov, G. Antchev, R. Hadjiiska, P. Iaydjiev, M. Misheva, M. Rodozov, M. Shopova, G. Sultanov

University of Sofia, Sofia, Bulgaria
A. Dimitrov, T. Ivanov, L. Litov, B. Pavlov, P. Petkov, A. Petrov

Beihang University, Beijing, China
T. Cheng, T. Javaid[7], M. Mittal, L. Yuan

Department of Physics, Tsinghua University, Beijing, China
M. Ahmad, G. Bauer, C. Dozen[8], Z. Hu, J. Martins[9], Y. Wang, K. Yi[10,11]

Institute of High Energy Physics, Beijing, China
E. Chapon, G.M. Chen[7], H.S. Chen[7], M. Chen, F. Iemmi, A. Kapoor, D. Leggat, H. Liao, Z.-A. Liu[7], V. Milosevic, F. Monti, R. Sharma, J. Tao, J. Thomas-Wilsker, J. Wang, H. Zhang, J. Zhao

State Key Laboratory of Nuclear Physics and Technology, Peking University, Beijing, China
A. Agapitos, Y. An, Y. Ban, C. Chen, A. Levin, Q. Li, X. Lyu, Y. Mao, S.J. Qian, D. Wang, Q. Wang, J. Xiao

Sun Yat-Sen University, Guangzhou, China
M. Lu, Z. You

Institute of Modern Physics and Key Laboratory of Nuclear Physics and Ion-beam Application (MOE) - Fudan University, Shanghai, China
X. Gao[3], H. Okawa, Y. Zhang

Zhejiang University, Hangzhou, China, Zhejiang, China
Z. Lin, M. Xiao

Universidad de Los Andes, Bogota, Colombia
C. Avila, A. Cabrera, C. Florez, J. Fraga

Universidad de Antioquia, Medellin, Colombia
J. Mejia Guisao, F. Ramirez, J.D. Ruiz Alvarez, C.A. Salazar González

University of Split, Faculty of Electrical Engineering, Mechanical Engineering and Naval Architecture, Split, Croatia
D. Giljanovic, N. Godinovic, D. Lelas, I. Puljak

University of Split, Faculty of Science, Split, Croatia
Z. Antunovic, M. Kovac, T. Sculac

Institute Rudjer Boskovic, Zagreb, Croatia
V. Brigljevic, D. Ferencek, D. Majumder, M. Roguljic, A. Starodumov[12], T. Susa

University of Cyprus, Nicosia, Cyprus
A. Attikis, K. Christoforou, E. Erodotou, A. Ioannou, G. Kole, M. Kolosova, S. Konstantinou, J. Mousa, C. Nicolaou, F. Ptochos, P.A. Razis, H. Rykaczewski, H. Saka

Charles University, Prague, Czech Republic
M. Finger[13], M. Finger Jr.[13], A. Kveton

Escuela Politecnica Nacional, Quito, Ecuador
E. Ayala

Universidad San Francisco de Quito, Quito, Ecuador
E. Carrera Jarrin

Academy of Scientific Research and Technology of the Arab Republic of Egypt, Egyp-

tian Network of High Energy Physics, Cairo, Egypt
S. Khalil[14], E. Salama[15,16]

Center for High Energy Physics (CHEP-FU), Fayoum University, El-Fayoum, Egypt
A. Lotfy, M.A. Mahmoud

National Institute of Chemical Physics and Biophysics, Tallinn, Estonia
S. Bhowmik, R.K. Dewanjee, K. Ehataht, M. Kadastik, S. Nandan, C. Nielsen, J. Pata, M. Raidal, L. Tani, C. Veelken

Department of Physics, University of Helsinki, Helsinki, Finland
P. Eerola, L. Forthomme, H. Kirschenmann, K. Osterberg, M. Voutilainen

Helsinki Institute of Physics, Helsinki, Finland
S. Bharthuar, E. Brücken, F. Garcia, J. Havukainen, M.S. Kim, R. Kinnunen, T. Lampén, K. Lassila-Perini, S. Lehti, T. Lindén, M. Lotti, L. Martikainen, M. Myllymäki, J. Ott, H. Siikonen, E. Tuominen, J. Tuominiemi

Lappeenranta University of Technology, Lappeenranta, Finland
P. Luukka, H. Petrow, T. Tuuva

IRFU, CEA, Université Paris-Saclay, Gif-sur-Yvette, France
C. Amendola, M. Besancon, F. Couderc, M. Dejardin, D. Denegri, J.L. Faure, F. Ferri, S. Ganjour, P. Gras, G. Hamel de Monchenault, P. Jarry, B. Lenzi, E. Locci, J. Malcles, J. Rander, A. Rosowsky, M.Ö. Sahin, A. Savoy-Navarro[17], M. Titov, G.B. Yu

Laboratoire Leprince-Ringuet, CNRS/IN2P3, Ecole Polytechnique, Institut Polytechnique de Paris, Palaiseau, France
S. Ahuja, F. Beaudette, M. Bonanomi, A. Buchot Perraguin, P. Busson, A. Cappati, C. Charlot, O. Davignon, B. Diab, G. Falmagne, S. Ghosh, R. Granier de Cassagnac, A. Hakimi, I. Kucher, J. Motta, M. Nguyen, C. Ochando, P. Paganini, J. Rembser, R. Salerno, U. Sarkar, J.B. Sauvan, Y. Sirois, A. Tarabini, A. Zabi, A. Zghiche

Université de Strasbourg, CNRS, IPHC UMR 7178, Strasbourg, France
J.-L. Agram[18], J. Andrea, D. Apparu, D. Bloch, G. Bourgatte, J.-M. Brom, E.C. Chabert, C. Collard, D. Darej, J.-C. Fontaine[18], U. Goerlach, C. Grimault, A.-C. Le Bihan, E. Nibigira, P. Van Hove

Institut de Physique des 2 Infinis de Lyon (IP2I), Villeurbanne, France
E. Asilar, S. Beauceron, C. Bernet, G. Boudoul, C. Camen, A. Carle, N. Chanon, D. Contardo, P. Depasse, H. El Mamouni, J. Fay, S. Gascon, M. Gouzevitch, B. Ille, I.B. Laktineh, H. Lattaud, A. Lesauvage, M. Lethuillier, L. Mirabito, S. Perries, K. Shchablo, V. Sordini, L. Torterotot, G. Touquet, M. Vander Donckt, S. Viret

Georgian Technical University, Tbilisi, Georgia
I. Bagaturia[19], I. Lomidze, Z. Tsamalaidze[13]

RWTH Aachen University, I. Physikalisches Institut, Aachen, Germany
V. Botta, L. Feld, K. Klein, M. Lipinski, D. Meuser, A. Pauls, N. Röwert, J. Schulz, M. Teroerde

RWTH Aachen University, III. Physikalisches Institut A, Aachen, Germany
A. Dodonova, D. Eliseev, M. Erdmann, P. Fackeldey, B. Fischer, S. Ghosh, T. Hebbeker, K. Hoepfner, F. Ivone, L. Mastrolorenzo, M. Merschmeyer, A. Meyer, G. Mocellin, S. Mondal, S. Mukherjee, D. Noll, A. Novak, T. Pook, A. Pozdnyakov,

Y. Rath, H. Reithler, J. Roemer, A. Schmidt, S.C. Schuler, A. Sharma, L. Vigilante, S. Wiedenbeck, S. Zaleski

RWTH Aachen University, III. Physikalisches Institut B, Aachen, Germany
C. Dziwok, G. Flügge, W. Haj Ahmad[20], O. Hlushchenko, T. Kress, A. Nowack, C. Pistone, O. Pooth, D. Roy, H. Sert, A. Stahl[21], T. Ziemons, A. Zotz

Deutsches Elektronen-Synchrotron, Hamburg, Germany
H. Aarup Petersen, M. Aldaya Martin, P. Asmuss, S. Baxter, M. Bayatmakou, O. Behnke, A. Bermúdez Martínez, S. Bhattacharya, A.A. Bin Anuar, K. Borras[22], D. Brunner, A. Campbell, A. Cardini, C. Cheng, F. Colombina, S. Consuegra Rodríguez, G. Correia Silva, V. Danilov, M. De Silva, L. Didukh, G. Eckerlin, D. Eckstein, L.I. Estevez Banos, O. Filatov, E. Gallo[23], A. Geiser, A. Giraldi, A. Grohsjean, M. Guthoff, A. Jafari[24], N.Z. Jomhari, H. Jung, A. Kasem[22], M. Kasemann, H. Kaveh, C. Kleinwort, D. Krücker, W. Lange, J. Lidrych, K. Lipka, W. Lohmann[25], R. Mankel, I.-A. Melzer-Pellmann, M. Mendizabal Morentin, J. Metwally, A.B. Meyer, M. Meyer, J. Mnich, A. Mussgiller, Y. Otarid, D. Pérez Adán, D. Pitzl, A. Raspereza, B. Ribeiro Lopes, J. Rübenach, A. Saggio, A. Saibel, M. Savitskyi, M. Scham[26], V. Scheurer, S. Schnake, P. Schütze, C. Schwanenberger[23], M. Shchedrolosiev, R.E. Sosa Ricardo, D. Stafford, N. Tonon, M. Van De Klundert, R. Walsh, D. Walter, Y. Wen, K. Wichmann, L. Wiens, C. Wissing, S. Wuchterl

University of Hamburg, Hamburg, Germany
R. Aggleton, S. Albrecht, S. Bein, L. Benato, P. Connor, K. De Leo, M. Eich, F. Feindt, A. Fröhlich, C. Garbers, E. Garutti, P. Gunnellini, M. Hajheidari, J. Haller, A. Hinzmann, G. Kasieczka, R. Klanner, R. Kogler, T. Kramer, V. Kutzner, J. Lange, T. Lange, A. Lobanov, A. Malara, A. Nigamova, K.J. Pena Rodriguez, O. Rieger, P. Schleper, M. Schröder, J. Schwandt, J. Sonneveld, H. Stadie, G. Steinbrück, A. Tews, I. Zoi

Karlsruher Institut fuer Technologie, Karlsruhe, Germany
J. Bechtel, S. Brommer, M. Burkart, E. Butz, R. Caspart, T. Chwalek, W. De Boer[†], A. Dierlamm, A. Droll, K. El Morabit, N. Faltermann, M. Giffels, J.o. Gosewisch, A. Gottmann, F. Hartmann[21], C. Heidecker, U. Husemann, P. Keicher, R. Koppenhöfer, S. Maier, M. Metzler, S. Mitra, Th. Müller, M. Neukum, A. Nürnberg, G. Quast, K. Rabbertz, J. Rauser, D. Savoiu, M. Schnepf, D. Seith, I. Shvetsov, H.J. Simonis, R. Ulrich, J. Van Der Linden, R.F. Von Cube, M. Wassmer, M. Weber, S. Wieland, R. Wolf, S. Wozniewski, S. Wunsch

Institute of Nuclear and Particle Physics (INPP), NCSR Demokritos, Aghia Paraskevi, Greece
G. Anagnostou, G. Daskalakis, T. Geralis, A. Kyriakis, D. Loukas, A. Stakia

National and Kapodistrian University of Athens, Athens, Greece
M. Diamantopoulou, D. Karasavvas, G. Karathanasis, P. Kontaxakis, C.K. Koraka, A. Manousakis-Katsikakis, A. Panagiotou, I. Papavergou, N. Saoulidou, K. Theofilatos, E. Tziaferi, K. Vellidis, E. Vourliotis

National Technical University of Athens, Athens, Greece
G. Bakas, K. Kousouris, I. Papakrivopoulos, G. Tsipolitis, A. Zacharopoulou

University of Ioánnina, Ioánnina, Greece
K. Adamidis, I. Bestintzanos, I. Evangelou, C. Foudas, P. Gianneios, P. Katsoulis, P. Kokkas,

N. Manthos, I. Papadopoulos, J. Strologas

MTA-ELTE Lendület CMS Particle and Nuclear Physics Group, Eötvös Loránd University, Budapest, Hungary
M. Csanad, K. Farkas, M.M.A. Gadallah[27], S. Lökös[28], P. Major, K. Mandal, A. Mehta, G. Pasztor, A.J. Rádl, O. Surányi, G.I. Veres

Wigner Research Centre for Physics, Budapest, Hungary
M. Bartók[29], G. Bencze, C. Hajdu, D. Horvath[30], F. Sikler, V. Veszpremi

Institute of Nuclear Research ATOMKI, Debrecen, Hungary
S. Czellar, D. Fasanella, J. Karancsi[29], J. Molnar, Z. Szillasi, D. Teyssier

Institute of Physics, University of Debrecen, Debrecen, Hungary
P. Raics, Z.L. Trocsanyi[31], B. Ujvari

Karoly Robert Campus, MATE Institute of Technology, Gyongyos, Hungary
T. Csorgo[32], F. Nemes[32], T. Novak

Indian Institute of Science (IISc), Bangalore, India
S. Choudhury, J.R. Komaragiri, D. Kumar, L. Panwar, P.C. Tiwari

National Institute of Science Education and Research, HBNI, Bhubaneswar, India
S. Bahinipati[33], C. Kar, P. Mal, T. Mishra, V.K. Muraleedharan Nair Bindhu[34], A. Nayak[34], P. Saha, N. Sur, S.K. Swain, D. Vats[34]

Panjab University, Chandigarh, India
S. Bansal, S.B. Beri, V. Bhatnagar, G. Chaudhary, S. Chauhan, N. Dhingra[35], R. Gupta, A. Kaur, M. Kaur, S. Kaur, P. Kumari, M. Meena, K. Sandeep, J.B. Singh, A.K. Virdi

University of Delhi, Delhi, India
A. Ahmed, A. Bhardwaj, B.C. Choudhary, M. Gola, S. Keshri, A. Kumar, M. Naimuddin, P. Priyanka, K. Ranjan, A. Shah

Saha Institute of Nuclear Physics, HBNI, Kolkata, India
M. Bharti[36], R. Bhattacharya, S. Bhattacharya, D. Bhowmik, S. Dutta, S. Dutta, B. Gomber[37], M. Maity[38], P. Palit, P.K. Rout, G. Saha, B. Sahu, S. Sarkar, M. Sharan, B. Singh[36], S. Thakur[36]

Indian Institute of Technology Madras, Madras, India
P.K. Behera, S.C. Behera, P. Kalbhor, A. Muhammad, R. Pradhan, P.R. Pujahari, A. Sharma, A.K. Sikdar

Bhabha Atomic Research Centre, Mumbai, India
D. Dutta, V. Jha, V. Kumar, D.K. Mishra, K. Naskar[39], P.K. Netrakanti, L.M. Pant, P. Shukla

Tata Institute of Fundamental Research-A, Mumbai, India
T. Aziz, S. Dugad, M. Kumar

Tata Institute of Fundamental Research-B, Mumbai, India
S. Banerjee, R. Chudasama, M. Guchait, S. Karmakar, S. Kumar, G. Majumder, K. Mazumdar, S. Mukherjee

Indian Institute of Science Education and Research (IISER), Pune, India
K. Alpana, S. Dube, B. Kansal, A. Laha, S. Pandey, A. Rane, A. Rastogi, S. Sharma

Isfahan University of Technology, Isfahan, Iran
H. Bakhshiansohi[40], E. Khazaie, M. Zeinali[41]

Institute for Research in Fundamental Sciences (IPM), Tehran, Iran
S. Chenarani[42], S.M. Etesami, M. Khakzad, M. Mohammadi Najafabadi

University College Dublin, Dublin, Ireland
M. Grunewald

INFN Sezione di Bari [a], Bari, Italy, Università di Bari [b], Bari, Italy, Politecnico di Bari [c], Bari, Italy
M. Abbrescia[a,b], R. Aly[a,b,43], C. Aruta[a,b], A. Colaleo[a], D. Creanza[a,c], N. De Filippis[a,c], M. De Palma[a,b], A. Di Florio[a,b], A. Di Pilato[a,b], W. Elmetenawee[a,b], L. Fiore[a], A. Gelmi[a,b], M. Gul[a], G. Iaselli[a,c], M. Ince[a,b], S. Lezki[a,b], G. Maggi[a,c], M. Maggi[a], I. Margjeka[a,b], V. Mastrapasqua[a,b], S. My[a,b], S. Nuzzo[a,b], A. Pellecchia[a,b], A. Pompili[a,b], G. Pugliese[a,c], D. Ramos[a], A. Ranieri[a], G. Selvaggi[a,b], L. Silvestris[a], F.M. Simone[a,b], Ü. Sözbilir[a], R. Venditti[a], P. Verwilligen[a]

INFN Sezione di Bologna [a], Bologna, Italy, Università di Bologna [b], Bologna, Italy
G. Abbiendi[a], C. Battilana[a,b], D. Bonacorsi[a,b], L. Borgonovi[a], L. Brigliadori[a], R. Campanini[a,b], P. Capiluppi[a,b], A. Castro[a,b], F.R. Cavallo[a], M. Cuffiani[a,b], G.M. Dallavalle[a], T. Diotalevi[a,b], F. Fabbri[a], A. Fanfani[a,b], P. Giacomelli[a], L. Giommi[a,b], C. Grandi[a], L. Guiducci[a,b], S. Lo Meo[a,44], L. Lunerti[a,b], S. Marcellini[a], G. Masetti[a], F.L. Navarria[a,b], A. Perrotta[a], F. Primavera[a,b], A.M. Rossi[a,b], T. Rovelli[a,b], G.P. Siroli[a,b]

INFN Sezione di Catania [a], Catania, Italy, Università di Catania [b], Catania, Italy
S. Albergo[a,b,45], S. Costa[a,b,45], A. Di Mattia[a], R. Potenza[a,b], A. Tricomi[a,b,45], C. Tuve[a,b]

INFN Sezione di Firenze [a], Firenze, Italy, Università di Firenze [b], Firenze, Italy
G. Barbagli[a], A. Cassese[a], R. Ceccarelli[a,b], V. Ciulli[a,b], C. Civinini[a], R. D'Alessandro[a,b], E. Focardi[a,b], G. Latino[a,b], P. Lenzi[a,b], M. Lizzo[a,b], M. Meschini[a], S. Paoletti[a], R. Seidita[a,b], G. Sguazzoni[a], L. Viliani[a]

INFN Laboratori Nazionali di Frascati, Frascati, Italy
L. Benussi, S. Bianco, D. Piccolo

INFN Sezione di Genova [a], Genova, Italy, Università di Genova [b], Genova, Italy
M. Bozzo[a,b], F. Ferro[a], R. Mulargia[a,b], E. Robutti[a], S. Tosi[a,b]

INFN Sezione di Milano-Bicocca [a], Milano, Italy, Università di Milano-Bicocca [b], Milano, Italy
A. Benaglia[a], G. Boldrini, F. Brivio[a,b], F. Cetorelli[a,b], F. De Guio[a,b], M.E. Dinardo[a,b], P. Dini[a], S. Gennai[a], A. Ghezzi[a,b], P. Govoni[a,b], L. Guzzi[a,b], M.T. Lucchini[a,b], M. Malberti[a], S. Malvezzi[a], A. Massironi[a], D. Menasce[a], L. Moroni[a], M. Paganoni[a,b], D. Pedrini[a], B.S. Pinolini, S. Ragazzi[a,b], N. Redaelli[a], T. Tabarelli de Fatis[a,b], D. Valsecchi[a,b,21], D. Zuolo[a,b]

INFN Sezione di Napoli [a], Napoli, Italy, Università di Napoli 'Federico II' [b], Napoli, Italy, Università della Basilicata [c], Potenza, Italy, Università G. Marconi [d], Roma, Italy
S. Buontempo[a], F. Carnevali[a,b], N. Cavallo[a,c], A. De Iorio[a,b], F. Fabozzi[a,c], A.O.M. Iorio[a,b], L. Lista[a,b], S. Meola[a,d,21], P. Paolucci[a,21], B. Rossi[a], C. Sciacca[a,b]

INFN Sezione di Padova [a], Padova, Italy, Università di Padova [b], Padova, Italy, Università

di Trento [c], Trento, Italy
P. Azzi[a], N. Bacchetta[a], D. Bisello[a,b], P. Bortignon[a], A. Bragagnolo[a,b], R. Carlin[a,b], P. Checchia[a], T. Dorigo[a], U. Dosselli[a], F. Gasparini[a,b], U. Gasparini[a,b], G. Grosso, S.Y. Hoh[a,b], L. Layer[a,46], E. Lusiani, M. Margoni[a,b], A.T. Meneguzzo[a,b], J. Pazzini[a,b], P. Ronchese[a,b], R. Rossin[a,b], F. Simonetto[a,b], G. Strong[a], M. Tosi[a,b], H. Yarar[a,b], M. Zanetti[a,b], P. Zotto[a,b], A. Zucchetta[a,b], G. Zumerle[a,b]

INFN Sezione di Pavia [a], Pavia, Italy, Università di Pavia [b], Pavia, Italy
C. Aime'[a,b], A. Braghieri[a], S. Calzaferri[a,b], D. Fiorina[a,b], P. Montagna[a,b], S.P. Ratti[a,b], V. Re[a], C. Riccardi[a,b], P. Salvini[a], I. Vai[a], P. Vitulo[a,b]

INFN Sezione di Perugia [a], Perugia, Italy, Università di Perugia [b], Perugia, Italy
P. Asenov[a,47], G.M. Bilei[a], D. Ciangottini[a,b], L. Fanò[a,b], P. Lariccia[a,b], M. Magherini[b], G. Mantovani[a,b], V. Mariani[a,b], M. Menichelli[a], F. Moscatelli[a,47], A. Piccinelli[a,b], M. Presilla[a,b], A. Rossi[a,b], A. Santocchia[a,b], D. Spiga[a], T. Tedeschi[a,b]

INFN Sezione di Pisa [a], Pisa, Italy, Università di Pisa [b], Pisa, Italy, Scuola Normale Superiore di Pisa [c], Pisa, Italy, Università di Siena [d], Siena, Italy
P. Azzurri[a], G. Bagliesi[a], V. Bertacchi[a,c], L. Bianchini[a], T. Boccali[a], E. Bossini[a,b], R. Castaldi[a], M.A. Ciocci[a,b], V. D'Amante[a,d], R. Dell'Orso[a], M.R. Di Domenico[a,d], S. Donato[a], A. Giassi[a], F. Ligabue[a,c], E. Manca[a,c], G. Mandorli[a,c], D. Matos Figueiredo, A. Messineo[a,b], F. Palla[a], S. Parolia[a,b], G. Ramirez-Sanchez[a,c], A. Rizzi[a,b], G. Rolandi[a,c], S. Roy Chowdhury[a,c], A. Scribano[a], N. Shafiei[a,b], P. Spagnolo[a], R. Tenchini[a], G. Tonelli[a,b], N. Turini[a,d], A. Venturi[a], P.G. Verdini[a]

INFN Sezione di Roma [a], Rome, Italy, Sapienza Università di Roma [b], Rome, Italy
P. Barria[a], M. Campana[a,b], F. Cavallari[a], D. Del Re[a,b], E. Di Marco[a], M. Diemoz[a], E. Longo[a,b], P. Meridiani[a], G. Organtini[a,b], F. Pandolfi[a], R. Paramatti[a,b], C. Quaranta[a,b], S. Rahatlou[a,b], C. Rovelli[a], F. Santanastasio[a,b], L. Soffi[a], R. Tramontano[a,b]

INFN Sezione di Torino [a], Torino, Italy, Università di Torino [b], Torino, Italy, Università del Piemonte Orientale [c], Novara, Italy
N. Amapane[a,b], R. Arcidiacono[a,c], S. Argiro[a,b], M. Arneodo[a,c], N. Bartosik[a], R. Bellan[a,b], A. Bellora[a,b], J. Berenguer Antequera[a,b], C. Biino[a], N. Cartiglia[a], S. Cometti[a], M. Costa[a,b], R. Covarelli[a,b], N. Demaria[a], B. Kiani[a,b], F. Legger[a], C. Mariotti[a], S. Maselli[a], E. Migliore[a,b], E. Monteil[a,b], M. Monteno[a], M.M. Obertino[a,b], G. Ortona[a], L. Pacher[a,b], N. Pastrone[a], M. Pelliccioni[a], G.L. Pinna Angioni[a,b], M. Ruspa[a,c], K. Shchelina[a], F. Siviero[a,b], V. Sola[a], A. Solano[a,b], D. Soldi[a,b], A. Staiano[a], M. Tornago[a,b], D. Trocino[a], A. Vagnerini[a,b]

INFN Sezione di Trieste [a], Trieste, Italy, Università di Trieste [b], Trieste, Italy
S. Belforte[a], V. Candelise[a,b], M. Casarsa[a], F. Cossutti[a], A. Da Rold[a,b], G. Della Ricca[a,b], G. Sorrentino[a,b], F. Vazzoler[a,b]

Kyungpook National University, Daegu, Korea
S. Dogra, C. Huh, B. Kim, D.H. Kim, G.N. Kim, J. Kim, J. Lee, S.W. Lee, C.S. Moon, Y.D. Oh, S.I. Pak, B.C. Radburn-Smith, S. Sekmen, Y.C. Yang

Chonnam National University, Institute for Universe and Elementary Particles, Kwangju, Korea
H. Kim, D.H. Moon

Hanyang University, Seoul, Korea
B. Francois, T.J. Kim, J. Park

Korea University, Seoul, Korea
S. Cho, S. Choi, Y. Go, B. Hong, K. Lee, K.S. Lee, J. Lim, J. Park, S.K. Park, J. Yoo

Kyung Hee University, Department of Physics, Seoul, Republic of Korea, Seoul, Korea
J. Goh, A. Gurtu

Sejong University, Seoul, Korea
H.S. Kim, Y. Kim

Seoul National University, Seoul, Korea
J. Almond, J.H. Bhyun, J. Choi, S. Jeon, J. Kim, J.S. Kim, S. Ko, H. Kwon, H. Lee, S. Lee, B.H. Oh, M. Oh, S.B. Oh, H. Seo, U.K. Yang, I. Yoon

University of Seoul, Seoul, Korea
W. Jang, D.Y. Kang, Y. Kang, S. Kim, B. Ko, J.S.H. Lee, Y. Lee, J.A. Merlin, I.C. Park, Y. Roh, M.S. Ryu, D. Song, I.J. Watson, S. Yang

Yonsei University, Department of Physics, Seoul, Korea
S. Ha, H.D. Yoo

Sungkyunkwan University, Suwon, Korea
M. Choi, H. Lee, Y. Lee, I. Yu

College of Engineering and Technology, American University of the Middle East (AUM), Egaila, Kuwait, Dasman, Kuwait
T. Beyrouthy, Y. Maghrbi

Riga Technical University, Riga, Latvia
K. Dreimanis, V. Veckalns[48]

Vilnius University, Vilnius, Lithuania
M. Ambrozas, A. Carvalho Antunes De Oliveira, A. Juodagalvis, A. Rinkevicius, G. Tamulaitis

National Centre for Particle Physics, Universiti Malaya, Kuala Lumpur, Malaysia
N. Bin Norjoharuddeen, W.A.T. Wan Abdullah, M.N. Yusli, Z. Zolkapli

Universidad de Sonora (UNISON), Hermosillo, Mexico
J.F. Benitez, A. Castaneda Hernandez, M. León Coello, J.A. Murillo Quijada, A. Sehrawat, L. Valencia Palomo

Centro de Investigacion y de Estudios Avanzados del IPN, Mexico City, Mexico
G. Ayala, H. Castilla-Valdez, E. De La Cruz-Burelo, I. Heredia-De La Cruz[49], R. Lopez-Fernandez, C.A. Mondragon Herrera, D.A. Perez Navarro, A. Sánchez Hernández

Universidad Iberoamericana, Mexico City, Mexico
S. Carrillo Moreno, C. Oropeza Barrera, F. Vazquez Valencia

Benemerita Universidad Autonoma de Puebla, Puebla, Mexico
I. Pedraza, H.A. Salazar Ibarguen, C. Uribe Estrada

University of Montenegro, Podgorica, Montenegro
J. Mijuskovic[50], N. Raicevic

University of Auckland, Auckland, New Zealand

D. Krofcheck

University of Canterbury, Christchurch, New Zealand
P.H. Butler, P. Lujan

National Centre for Physics, Quaid-I-Azam University, Islamabad, Pakistan
A. Ahmad, M.I. Asghar, A. Awais, M.I.M. Awan, H.R. Hoorani, W.A. Khan, M.A. Shah, M. Shoaib, M. Waqas

AGH University of Science and Technology Faculty of Computer Science, Electronics and Telecommunications, Krakow, Poland
V. Avati, L. Grzanka, M. Malawski

National Centre for Nuclear Research, Swierk, Poland
H. Bialkowska, M. Bluj, B. Boimska, M. Górski, M. Kazana, M. Szleper, P. Zalewski

Institute of Experimental Physics, Faculty of Physics, University of Warsaw, Warsaw, Poland
K. Bunkowski, K. Doroba, A. Kalinowski, M. Konecki, J. Krolikowski

Laboratório de Instrumentação e Física Experimental de Partículas, Lisboa, Portugal
M. Araujo, P. Bargassa, D. Bastos, A. Boletti, P. Faccioli, M. Gallinaro, J. Hollar, N. Leonardo, T. Niknejad, M. Pisano, J. Seixas, O. Toldaiev, J. Varela

Joint Institute for Nuclear Research, Dubna, Russia
S. Afanasiev, D. Budkouski, I. Golutvin, I. Gorbunov, V. Karjavine, V. Korenkov, A. Lanev, A. Malakhov, V. Matveev[51,52], V. Palichik, V. Perelygin, M. Savina, D. Seitova, V. Shalaev, S. Shmatov, S. Shulha, V. Smirnov, O. Teryaev, N. Voytishin, B.S. Yuldashev[53], A. Zarubin, I. Zhizhin

Petersburg Nuclear Physics Institute, Gatchina (St. Petersburg), Russia
G. Gavrilov, V. Golovtcov, Y. Ivanov, V. Kim[54], E. Kuznetsova[55], V. Murzin, V. Oreshkin, I. Smirnov, D. Sosnov, V. Sulimov, L. Uvarov, S. Volkov, A. Vorobyev

Institute for Nuclear Research, Moscow, Russia
Yu. Andreev, A. Dermenev, S. Gninenko, N. Golubev, A. Karneyeu, D. Kirpichnikov, M. Kirsanov, N. Krasnikov, A. Pashenkov, G. Pivovarov, A. Toropin

Institute for Theoretical and Experimental Physics named by A.I. Alikhanov of NRC 'Kurchatov Institute', Moscow, Russia
V. Epshteyn, V. Gavrilov, N. Lychkovskaya, A. Nikitenko[56], V. Popov, A. Stepennov, M. Toms, E. Vlasov, A. Zhokin

Moscow Institute of Physics and Technology, Moscow, Russia
T. Aushev

National Research Nuclear University 'Moscow Engineering Physics Institute' (MEPhI), Moscow, Russia
O. Bychkova, R. Chistov[57], M. Danilov[58], A. Oskin, P. Parygin, S. Polikarpov[57]

P.N. Lebedev Physical Institute, Moscow, Russia
V. Andreev, M. Azarkin, I. Dremin, M. Kirakosyan, A. Terkulov

Skobeltsyn Institute of Nuclear Physics, Lomonosov Moscow State University, Moscow, Russia
A. Belyaev, E. Boos, V. Bunichev, M. Dubinin[59], L. Dudko, A. Ershov, A. Gribushin, V. Klyukhin, O. Kodolova, I. Lokhtin, S. Obraztsov, M. Perfilov, V. Savrin

Novosibirsk State University (NSU), Novosibirsk, Russia
V. Blinov[60], T. Dimova[60], L. Kardapoltsev[60], A. Kozyrev[60], I. Ovtin[60], O. Radchenko[60], Y. Skovpen[60]

Institute for High Energy Physics of National Research Centre 'Kurchatov Institute', Protvino, Russia
I. Azhgirey, I. Bayshev, D. Elumakhov, V. Kachanov, D. Konstantinov, P. Mandrik, V. Petrov, R. Ryutin, S. Slabospitskii, A. Sobol, S. Troshin, N. Tyurin, A. Uzunian, A. Volkov

National Research Tomsk Polytechnic University, Tomsk, Russia
A. Babaev, V. Okhotnikov

Tomsk State University, Tomsk, Russia
V. Borshch, V. Ivanchenko, E. Tcherniaev

University of Belgrade: Faculty of Physics and VINCA Institute of Nuclear Sciences, Belgrade, Serbia
P. Adzic[61], M. Dordevic, P. Milenovic, J. Milosevic

Centro de Investigaciones Energéticas Medioambientales y Tecnológicas (CIEMAT), Madrid, Spain
M. Aguilar-Benitez, J. Alcaraz Maestre, A. Álvarez Fernández, I. Bachiller, M. Barrio Luna, Cristina F. Bedoya, C.A. Carrillo Montoya, M. Cepeda, M. Cerrada, N. Colino, B. De La Cruz, A. Delgado Peris, J.P. Fernández Ramos, J. Flix, M.C. Fouz, O. Gonzalez Lopez, S. Goy Lopez, J.M. Hernandez, M.I. Josa, J. León Holgado, D. Moran, Á. Navarro Tobar, C. Perez Dengra, A. Pérez-Calero Yzquierdo, J. Puerta Pelayo, I. Redondo, L. Romero, S. Sánchez Navas, L. Urda Gómez, C. Willmott

Universidad Autónoma de Madrid, Madrid, Spain
J.F. de Trocóniz, R. Reyes-Almanza

Universidad de Oviedo, Instituto Universitario de Ciencias y Tecnologías Espaciales de Asturias (ICTEA), Oviedo, Spain
B. Alvarez Gonzalez, J. Cuevas, C. Erice, J. Fernandez Menendez, S. Folgueras, I. Gonzalez Caballero, J.R. González Fernández, E. Palencia Cortezon, C. Ramón Álvarez, V. Rodríguez Bouza, A. Soto Rodríguez, A. Trapote, N. Trevisani, C. Vico Villalba

Instituto de Física de Cantabria (IFCA), CSIC-Universidad de Cantabria, Santander, Spain
J.A. Brochero Cifuentes, I.J. Cabrillo, A. Calderon, J. Duarte Campderros, M. Fernandez, C. Fernandez Madrazo, P.J. Fernández Manteca, A. García Alonso, G. Gomez, C. Martinez Rivero, P. Martinez Ruiz del Arbol, F. Matorras, P. Matorras Cuevas, J. Piedra Gomez, C. Prieels, T. Rodrigo, A. Ruiz-Jimeno, L. Scodellaro, I. Vila, J.M. Vizan Garcia

University of Colombo, Colombo, Sri Lanka
M.K. Jayananda, B. Kailasapathy[62], D.U.J. Sonnadara, D.D.C. Wickramarathna

University of Ruhuna, Department of Physics, Matara, Sri Lanka
W.G.D. Dharmaratna, K. Liyanage, N. Perera, N. Wickramage

CERN, European Organization for Nuclear Research, Geneva, Switzerland
T.K. Aarrestad, D. Abbaneo, J. Alimena, E. Auffray, G. Auzinger, J. Baechler, P. Baillon[†], D. Barney, J. Bendavid, M. Bianco, A. Bocci, T. Camporesi, M. Capeans Garrido, G. Cerminara, N. Chernyavskaya, S.S. Chhibra, M. Cipriani, L. Cristella, D. d'Enterria, A. Dabrowski, A. David, A. De Roeck, M.M. Defranchis, M. Deile,

M. Dobson, M. Dünser, N. Dupont, A. Elliott-Peisert, N. Emriskova, F. Fallavollita[63], A. Florent, G. Franzoni, W. Funk, S. Giani, D. Gigi, K. Gill, F. Glege, L. Gouskos, M. Haranko, J. Hegeman, V. Innocente, T. James, P. Janot, J. Kaspar, J. Kieseler, M. Komm, N. Kratochwil, C. Lange, S. Laurila, P. Lecoq, A. Lintuluoto, K. Long, C. Lourenço, B. Maier, L. Malgeri, S. Mallios, M. Mannelli, A.C. Marini, F. Meijers, S. Mersi, E. Meschi, F. Moortgat, M. Mulders, S. Orfanelli, L. Orsini, F. Pantaleo, L. Pape, E. Perez, M. Peruzzi, A. Petrilli, G. Petrucciani, A. Pfeiffer, M. Pierini, D. Piparo, M. Pitt, H. Qu, T. Quast, D. Rabady, A. Racz, G. Reales Gutiérrez, M. Rieger, M. Rovere, H. Sakulin, J. Salfeld-Nebgen, S. Scarfi, C. Schäfer, C. Schwick, M. Selvaggi, A. Sharma, P. Silva, W. Snoeys, P. Sphicas[64], S. Summers, K. Tatar, V.R. Tavolaro, D. Treille, P. Tropea, A. Tsirou, G.P. Van Onsem, J. Wanczyk[65], K.A. Wozniak, W.D. Zeuner

Paul Scherrer Institut, Villigen, Switzerland
L. Caminada[66], A. Ebrahimi, W. Erdmann, R. Horisberger, Q. Ingram, H.C. Kaestli, D. Kotlinski, U. Langenegger, M. Missiroli[66], L. Noehte[66], T. Rohe

ETH Zurich - Institute for Particle Physics and Astrophysics (IPA), Zurich, Switzerland
K. Androsov[65], M. Backhaus, P. Berger, A. Calandri, A. De Cosa, G. Dissertori, M. Dittmar, M. Donegà, C. Dorfer, F. Eble, K. Gedia, F. Glessgen, T.A. Gómez Espinosa, C. Grab, D. Hits, W. Lustermann, A.-M. Lyon, R.A. Manzoni, L. Marchese, C. Martin Perez, M.T. Meinhard, F. Nessi-Tedaldi, J. Niedziela, F. Pauss, V. Perovic, S. Pigazzini, M.G. Ratti, M. Reichmann, C. Reissel, T. Reitenspiess, B. Ristic, D. Ruini, D.A. Sanz Becerra, V. Stampf, J. Steggemann[65], R. Wallny, D.H. Zhu

Universität Zürich, Zurich, Switzerland
C. Amsler[67], P. Bärtschi, C. Botta, D. Brzhechko, M.F. Canelli, K. Cormier, A. De Wit, R. Del Burgo, J.K. Heikkilä, M. Huwiler, W. Jin, A. Jofrehei, B. Kilminster, S. Leontsinis, S.P. Liechti, A. Macchiolo, P. Meiring, V.M. Mikuni, U. Molinatti, I. Neutelings, A. Reimers, P. Robmann, S. Sanchez Cruz, K. Schweiger, M. Senger, Y. Takahashi

National Central University, Chung-Li, Taiwan
C. Adloff[68], C.M. Kuo, W. Lin, A. Roy, T. Sarkar[38], S.S. Yu

National Taiwan University (NTU), Taipei, Taiwan
L. Ceard, Y. Chao, K.F. Chen, P.H. Chen, W.-S. Hou, Y.y. Li, R.-S. Lu, E. Paganis, A. Psallidas, A. Steen, H.y. Wu, E. Yazgan, P.r. Yu

Chulalongkorn University, Faculty of Science, Department of Physics, Bangkok, Thailand
B. Asavapibhop, C. Asawatangtrakuldee, N. Srimanobhas

Çukurova University, Physics Department, Science and Art Faculty, Adana, Turkey
F. Boran, S. Damarseckin[69], Z.S. Demiroglu, F. Dolek, I. Dumanoglu[70], E. Eskut, Y. Guler[71], E. Gurpinar Guler[71], C. Isik, O. Kara, A. Kayis Topaksu, U. Kiminsu, G. Onengut, K. Ozdemir[72], A. Polatoz, A.E. Simsek, B. Tali[73], U.G. Tok, S. Turkcapar, I.S. Zorbakir

Middle East Technical University, Physics Department, Ankara, Turkey
B. Isildak[74], G. Karapinar, K. Ocalan[75], M. Yalvac[76]

Bogazici University, Istanbul, Turkey
B. Akgun, I.O. Atakisi, E. Gülmez, M. Kaya[77], O. Kaya[78], Ö. Özçelik, S. Tekten[79], E.A. Yetkin[80]

Istanbul Technical University, Istanbul, Turkey
A. Cakir, K. Cankocak[70], Y. Komurcu, S. Sen[81]

Istanbul University, Istanbul, Turkey
S. Cerci[73], I. Hos[82], B. Kaynak, S. Ozkorucuklu, D. Sunar Cerci[73], C. Zorbilmez

Institute for Scintillation Materials of National Academy of Science of Ukraine, Kharkov, Ukraine
B. Grynyov

National Scientific Center, Kharkov Institute of Physics and Technology, Kharkov, Ukraine
L. Levchuk

University of Bristol, Bristol, United Kingdom
D. Anthony, E. Bhal, S. Bologna, J.J. Brooke, A. Bundock, E. Clement, D. Cussans, H. Flacher, J. Goldstein, G.P. Heath, H.F. Heath, L. Kreczko, B. Krikler, S. Paramesvaran, S. Seif El Nasr-Storey, V.J. Smith, N. Stylianou[83], K. Walkingshaw Pass, R. White

Rutherford Appleton Laboratory, Didcot, United Kingdom
K.W. Bell, A. Belyaev[84], C. Brew, R.M. Brown, D.J.A. Cockerill, C. Cooke, K.V. Ellis, K. Harder, S. Harper, M.-L. Holmberg[85], J. Linacre, K. Manolopoulos, D.M. Newbold, E. Olaiya, D. Petyt, T. Reis, T. Schuh, C.H. Shepherd-Themistocleous, I.R. Tomalin, T. Williams

Imperial College, London, United Kingdom
R. Bainbridge, P. Bloch, S. Bonomally, J. Borg, S. Breeze, O. Buchmuller, V. Cepaitis, G.S. Chahal[86], D. Colling, P. Dauncey, G. Davies, M. Della Negra, S. Fayer, G. Fedi, G. Hall, M.H. Hassanshahi, G. Iles, J. Langford, L. Lyons, A.-M. Magnan, S. Malik, A. Martelli, D.G. Monk, J. Nash[87], M. Pesaresi, D.M. Raymond, A. Richards, A. Rose, E. Scott, C. Seez, A. Shtipliyski, A. Tapper, K. Uchida, T. Virdee[21], M. Vojinovic, N. Wardle, S.N. Webb, D. Winterbottom

Brunel University, Uxbridge, United Kingdom
K. Coldham, J.E. Cole, A. Khan, P. Kyberd, I.D. Reid, L. Teodorescu, S. Zahid

Baylor University, Waco, Texas, USA
S. Abdullin, A. Brinkerhoff, B. Caraway, J. Dittmann, K. Hatakeyama, A.R. Kanuganti, B. McMaster, N. Pastika, M. Saunders, S. Sawant, C. Sutantawibul, J. Wilson

Catholic University of America, Washington, DC, USA
R. Bartek, A. Dominguez, R. Uniyal, A.M. Vargas Hernandez

The University of Alabama, Tuscaloosa, Alabama, USA
A. Buccilli, S.I. Cooper, D. Di Croce, S.V. Gleyzer, C. Henderson, C.U. Perez, P. Rumerio[88], C. West

Boston University, Boston, Massachusetts, USA
A. Akpinar, A. Albert, D. Arcaro, C. Cosby, Z. Demiragli, E. Fontanesi, D. Gastler, S. May, J. Rohlf, K. Salyer, D. Sperka, D. Spitzbart, I. Suarez, A. Tsatsos, S. Yuan, D. Zou

Brown University, Providence, Rhode Island, USA
G. Benelli, B. Burkle, X. Coubez[22], D. Cutts, M. Hadley, U. Heintz, J.M. Hogan[89],

T. KWON, G. Landsberg, K.T. Lau, D. Li, M. Lukasik, J. Luo, M. Narain, N. Pervan, S. Sagir[90], F. Simpson, E. Usai, W.Y. Wong, X. Yan, D. Yu, W. Zhang

University of California, Davis, Davis, California, USA
J. Bonilla, C. Brainerd, R. Breedon, M. Calderon De La Barca Sanchez, M. Chertok, J. Conway, P.T. Cox, R. Erbacher, G. Haza, F. Jensen, O. Kukral, R. Lander, M. Mulhearn, D. Pellett, B. Regnery, D. Taylor, Y. Yao, F. Zhang

University of California, Los Angeles, California, USA
M. Bachtis, R. Cousins, A. Datta, D. Hamilton, J. Hauser, M. Ignatenko, M.A. Iqbal, T. Lam, W.A. Nash, S. Regnard, D. Saltzberg, B. Stone, V. Valuev

University of California, Riverside, Riverside, California, USA
K. Burt, Y. Chen, R. Clare, J.W. Gary, M. Gordon, G. Hanson, G. Karapostoli, O.R. Long, N. Manganelli, M. Olmedo Negrete, W. Si, S. Wimpenny, Y. Zhang

University of California, San Diego, La Jolla, California, USA
J.G. Branson, P. Chang, S. Cittolin, S. Cooperstein, N. Deelen, D. Diaz, J. Duarte, R. Gerosa, L. Giannini, J. Guiang, R. Kansal, V. Krutelyov, R. Lee, J. Letts, M. Masciovecchio, F. Mokhtar, M. Pieri, B.V. Sathia Narayanan, V. Sharma, M. Tadel, A. Vartak, F. Würthwein, Y. Xiang, A. Yagil

University of California, Santa Barbara - Department of Physics, Santa Barbara, California, USA
N. Amin, C. Campagnari, M. Citron, A. Dorsett, V. Dutta, J. Incandela, M. Kilpatrick, J. Kim, B. Marsh, H. Mei, M. Oshiro, M. Quinnan, J. Richman, U. Sarica, F. Setti, J. Sheplock, D. Stuart, S. Wang

California Institute of Technology, Pasadena, California, USA
A. Bornheim, O. Cerri, I. Dutta, J.M. Lawhorn, N. Lu, J. Mao, H.B. Newman, T.Q. Nguyen, M. Spiropulu, J.R. Vlimant, C. Wang, S. Xie, Z. Zhang, R.Y. Zhu

Carnegie Mellon University, Pittsburgh, Pennsylvania, USA
J. Alison, S. An, M.B. Andrews, P. Bryant, T. Ferguson, A. Harilal, C. Liu, T. Mudholkar, M. Paulini, A. Sanchez, W. Terrill

University of Colorado Boulder, Boulder, Colorado, USA
J.P. Cumalat, W.T. Ford, A. Hassani, E. MacDonald, R. Patel, A. Perloff, C. Savard, K. Stenson, K.A. Ulmer, S.R. Wagner

Cornell University, Ithaca, New York, USA
J. Alexander, S. Bright-Thonney, X. Chen, Y. Cheng, D.J. Cranshaw, S. Hogan, J. Monroy, J.R. Patterson, D. Quach, J. Reichert, M. Reid, A. Ryd, W. Sun, J. Thom, P. Wittich, R. Zou

Fermi National Accelerator Laboratory, Batavia, Illinois, USA
M. Albrow, M. Alyari, G. Apollinari, A. Apresyan, A. Apyan, S. Banerjee, L.A.T. Bauerdick, D. Berry, J. Berryhill, P.C. Bhat, K. Burkett, J.N. Butler, A. Canepa, G.B. Cerati, H.W.K. Cheung, F. Chlebana, K.F. Di Petrillo, V.D. Elvira, Y. Feng, J. Freeman, Z. Gecse, L. Gray, D. Green, S. Grünendahl, O. Gutsche, R.M. Harris, R. Heller, T.C. Herwig, J. Hirschauer, B. Jayatilaka, S. Jindariani, M. Johnson, U. Joshi, T. Klijnsma, B. Klima, K.H.M. Kwok, S. Lammel, D. Lincoln, R. Lipton, T. Liu, C. Madrid, K. Maeshima, C. Mantilla, D. Mason, P. McBride, P. Merkel, S. Mrenna, S. Nahn, J. Ngadiuba, V. O'Dell, V. Papadimitriou, K. Pedro, C. Pena[59], O. Prokofyev,

F. Ravera, A. Reinsvold Hall, L. Ristori, E. Sexton-Kennedy, N. Smith, A. Soha, W.J. Spalding, L. Spiegel, S. Stoynev, J. Strait, L. Taylor, S. Tkaczyk, N.V. Tran, L. Uplegger, E.W. Vaandering, H.A. Weber

University of Florida, Gainesville, Florida, USA
D. Acosta, P. Avery, D. Bourilkov, L. Cadamuro, V. Cherepanov, F. Errico, R.D. Field, D. Guerrero, B.M. Joshi, M. Kim, E. Koenig, J. Konigsberg, A. Korytov, K.H. Lo, K. Matchev, N. Menendez, G. Mitselmakher, A. Muthirakalayil Madhu, N. Rawal, D. Rosenzweig, S. Rosenzweig, J. Rotter, K. Shi, J. Sturdy, J. Wang, E. Yigitbasi, X. Zuo

Florida State University, Tallahassee, Florida, USA
T. Adams, A. Askew, R. Habibullah, V. Hagopian, K.F. Johnson, R. Khurana, T. Kolberg, G. Martinez, H. Prosper, C. Schiber, O. Viazlo, R. Yohay, J. Zhang

Florida Institute of Technology, Melbourne, Florida, USA
M.M. Baarmand, S. Butalla, T. Elkafrawy[16], M. Hohlmann, R. Kumar Verma, D. Noonan, M. Rahmani, F. Yumiceva

University of Illinois at Chicago (UIC), Chicago, Illinois, USA
M.R. Adams, H. Becerril Gonzalez, R. Cavanaugh, S. Dittmer, O. Evdokimov, C.E. Gerber, D.A. Hangal, D.J. Hofman, A.H. Merrit, C. Mills, G. Oh, T. Roy, S. Rudrabhatla, M.B. Tonjes, N. Varelas, J. Viinikainen, X. Wang, Z. Wu, Z. Ye

The University of Iowa, Iowa City, Iowa, USA
M. Alhusseini, K. Dilsiz[91], R.P. Gandrajula, O.K. Köseyan, J.-P. Merlo, A. Mestvirishvili[92], J. Nachtman, H. Ogul[93], Y. Onel, A. Penzo, C. Snyder, E. Tiras[94]

Johns Hopkins University, Baltimore, Maryland, USA
O. Amram, B. Blumenfeld, L. Corcodilos, J. Davis, M. Eminizer, A.V. Gritsan, S. Kyriacou, P. Maksimovic, J. Roskes, M. Swartz, T.Á. Vámi

The University of Kansas, Lawrence, Kansas, USA
A. Abreu, J. Anguiano, C. Baldenegro Barrera, P. Baringer, A. Bean, A. Bylinkin, Z. Flowers, T. Isidori, S. Khalil, J. King, G. Krintiras, A. Kropivnitskaya, M. Lazarovits, C. Le Mahieu, C. Lindsey, J. Marquez, N. Minafra, M. Murray, M. Nickel, C. Rogan, C. Royon, R. Salvatico, S. Sanders, E. Schmitz, C. Smith, J.D. Tapia Takaki, Q. Wang, Z. Warner, J. Williams, G. Wilson

Kansas State University, Manhattan, Kansas, USA
S. Duric, A. Ivanov, K. Kaadze, D. Kim, Y. Maravin, T. Mitchell, A. Modak, K. Nam

Lawrence Livermore National Laboratory, Livermore, California, USA
F. Rebassoo, D. Wright

University of Maryland, College Park, Maryland, USA
E. Adams, A. Baden, O. Baron, A. Belloni, S.C. Eno, N.J. Hadley, S. Jabeen, R.G. Kellogg, T. Koeth, A.C. Mignerey, S. Nabili, C. Palmer, M. Seidel, A. Skuja, L. Wang, K. Wong

Massachusetts Institute of Technology, Cambridge, Massachusetts, USA
D. Abercrombie, G. Andreassi, R. Bi, W. Busza, I.A. Cali, Y. Chen, M. D'Alfonso, J. Eysermans, C. Freer, G. Gomez Ceballos, M. Goncharov, P. Harris, M. Hu, M. Klute, D. Kovalskyi, J. Krupa, Y.-J. Lee, C. Mironov, C. Paus, D. Rankin, C. Roland, G. Roland, Z. Shi, G.S.F. Stephans, J. Wang, Z. Wang, B. Wyslouch

University of Minnesota, Minneapolis, Minnesota, USA
R.M. Chatterjee, A. Evans, J. Hiltbrand, Sh. Jain, M. Krohn, Y. Kubota, J. Mans, M. Revering, R. Rusack, R. Saradhy, N. Schroeder, N. Strobbe, M.A. Wadud

University of Nebraska-Lincoln, Lincoln, Nebraska, USA
K. Bloom, M. Bryson, S. Chauhan, D.R. Claes, C. Fangmeier, L. Finco, F. Golf, C. Joo, I. Kravchenko, M. Musich, I. Reed, J.E. Siado, G.R. Snow[†], W. Tabb, F. Yan, A.G. Zecchinelli

State University of New York at Buffalo, Buffalo, New York, USA
G. Agarwal, H. Bandyopadhyay, L. Hay, I. Iashvili, A. Kharchilava, C. McLean, D. Nguyen, J. Pekkanen, S. Rappoccio, A. Williams

Northeastern University, Boston, Massachusetts, USA
G. Alverson, E. Barberis, Y. Haddad, A. Hortiangtham, J. Li, G. Madigan, B. Marzocchi, D.M. Morse, V. Nguyen, T. Orimoto, A. Parker, L. Skinnari, A. Tishelman-Charny, T. Wamorkar, B. Wang, A. Wisecarver, D. Wood

Northwestern University, Evanston, Illinois, USA
S. Bhattacharya, J. Bueghly, Z. Chen, A. Gilbert, T. Gunter, K.A. Hahn, Y. Liu, N. Odell, M.H. Schmitt, M. Velasco

University of Notre Dame, Notre Dame, Indiana, USA
R. Band, R. Bucci, M. Cremonesi, A. Das, N. Dev, R. Goldouzian, M. Hildreth, K. Hurtado Anampa, C. Jessop, K. Lannon, J. Lawrence, N. Loukas, D. Lutton, N. Marinelli, I. Mcalister, T. McCauley, C. Mcgrady, K. Mohrman, C. Moore, Y. Musienko[51], R. Ruchti, P. Siddireddy, A. Townsend, M. Wayne, A. Wightman, M. Zarucki, L. Zygala

The Ohio State University, Columbus, Ohio, USA
B. Bylsma, B. Cardwell, L.S. Durkin, B. Francis, C. Hill, M. Nunez Ornelas, K. Wei, B.L. Winer, B.R. Yates

Princeton University, Princeton, New Jersey, USA
F.M. Addesa, B. Bonham, P. Das, G. Dezoort, P. Elmer, A. Frankenthal, B. Greenberg, N. Haubrich, S. Higginbotham, A. Kalogeropoulos, G. Kopp, S. Kwan, D. Lange, D. Marlow, K. Mei, I. Ojalvo, J. Olsen, D. Stickland, C. Tully

University of Puerto Rico, Mayaguez, Puerto Rico, USA
S. Malik, S. Norberg

Purdue University, West Lafayette, Indiana, USA
A.S. Bakshi, V.E. Barnes, R. Chawla, S. Das, L. Gutay, M. Jones, A.W. Jung, S. Karmarkar, D. Kondratyev, M. Liu, G. Negro, N. Neumeister, G. Paspalaki, S. Piperov, A. Purohit, J.F. Schulte, M. Stojanovic[17], J. Thieman, F. Wang, R. Xiao, W. Xie

Purdue University Northwest, Hammond, Indiana, USA
J. Dolen, N. Parashar

Rice University, Houston, Texas, USA
A. Baty, T. Carnahan, M. Decaro, S. Dildick, K.M. Ecklund, S. Freed, P. Gardner, F.J.M. Geurts, A. Kumar, W. Li, B.P. Padley, R. Redjimi, W. Shi, A.G. Stahl Leiton, S. Yang, L. Zhang[95], Y. Zhang

University of Rochester, Rochester, New York, USA
A. Bodek, P. de Barbaro, R. Demina, J.L. Dulemba, C. Fallon, T. Ferbel, M. Galanti,

A. Garcia-Bellido, O. Hindrichs, A. Khukhunaishvili, E. Ranken, R. Taus

Rutgers, The State University of New Jersey, Piscataway, New Jersey, USA
B. Chiarito, J.P. Chou, A. Gandrakota, Y. Gershtein, E. Halkiadakis, A. Hart, M. Heindl, O. Karacheban[25], I. Laflotte, A. Lath, R. Montalvo, K. Nash, M. Osherson, S. Salur, S. Schnetzer, S. Somalwar, R. Stone, S.A. Thayil, S. Thomas, H. Wang

University of Tennessee, Knoxville, Tennessee, USA
H. Acharya, A.G. Delannoy, S. Fiorendi, S. Spanier

Texas A&M University, College Station, Texas, USA
O. Bouhali[96], M. Dalchenko, A. Delgado, R. Eusebi, J. Gilmore, T. Huang, T. Kamon[97], H. Kim, S. Luo, S. Malhotra, R. Mueller, D. Overton, D. Rathjens, A. Safonov

Texas Tech University, Lubbock, Texas, USA
N. Akchurin, J. Damgov, V. Hegde, S. Kunori, K. Lamichhane, S.W. Lee, T. Mengke, S. Muthumuni, T. Peltola, I. Volobouev, Z. Wang, A. Whitbeck

Vanderbilt University, Nashville, Tennessee, USA
E. Appelt, S. Greene, A. Gurrola, W. Johns, A. Melo, H. Ni, K. Padeken, F. Romeo, P. Sheldon, S. Tuo, J. Velkovska

University of Virginia, Charlottesville, Virginia, USA
M.W. Arenton, B. Cox, G. Cummings, J. Hakala, R. Hirosky, M. Joyce, A. Ledovskoy, A. Li, C. Neu, C.E. Perez Lara, B. Tannenwald, S. White, E. Wolfe

Wayne State University, Detroit, Michigan, USA
N. Poudyal

University of Wisconsin - Madison, Madison, WI, Wisconsin, USA
K. Black, T. Bose, C. Caillol, S. Dasu, I. De Bruyn, P. Everaerts, F. Fienga, C. Galloni, H. He, M. Herndon, A. Hervé, U. Hussain, A. Lanaro, A. Loeliger, R. Loveless, J. Madhusudanan Sreekala, A. Mallampalli, A. Mohammadi, D. Pinna, A. Savin, V. Shang, V. Sharma, W.H. Smith, D. Teague, S. Trembath-Reichert, W. Vetens

†: Deceased
1: Also at TU Wien, Wien, Austria
2: Also at Institute of Basic and Applied Sciences, Faculty of Engineering, Arab Academy for Science, Technology and Maritime Transport, Alexandria, Egypt
3: Also at Université Libre de Bruxelles, Bruxelles, Belgium
4: Also at Universidade Estadual de Campinas, Campinas, Brazil
5: Also at Federal University of Rio Grande do Sul, Porto Alegre, Brazil
6: Also at The University of the State of Amazonas, Manaus, Brazil
7: Also at University of Chinese Academy of Sciences, Beijing, China
8: Also at Department of Physics, Tsinghua University, Beijing, China
9: Also at UFMS, Nova Andradina, Brazil
10: Also at Nanjing Normal University Department of Physics, Nanjing, China
11: Now at The University of Iowa, Iowa City, Iowa, USA
12: Also at Institute for Theoretical and Experimental Physics named by A.I. Alikhanov of NRC 'Kurchatov Institute', Moscow, Russia
13: Also at Joint Institute for Nuclear Research, Dubna, Russia
14: Also at Zewail City of Science and Technology, Zewail, Egypt
15: Also at British University in Egypt, Cairo, Egypt
16: Now at Ain Shams University, Cairo, Egypt

17: Also at Purdue University, West Lafayette, Indiana, USA
18: Also at Université de Haute Alsace, Mulhouse, France
19: Also at Ilia State University, Tbilisi, Georgia
20: Also at Erzincan Binali Yildirim University, Erzincan, Turkey
21: Also at CERN, European Organization for Nuclear Research, Geneva, Switzerland
22: Also at RWTH Aachen University, III. Physikalisches Institut A, Aachen, Germany
23: Also at University of Hamburg, Hamburg, Germany
24: Also at Isfahan University of Technology, Isfahan, Iran
25: Also at Brandenburg University of Technology, Cottbus, Germany
26: Also at Forschungszentrum Jülich, Juelich, Germany
27: Also at Physics Department, Faculty of Science, Assiut University, Assiut, Egypt
28: Also at Karoly Robert Campus, MATE Institute of Technology, Gyongyos, Hungary
29: Also at Institute of Physics, University of Debrecen, Debrecen, Hungary
30: Also at Institute of Nuclear Research ATOMKI, Debrecen, Hungary
31: Also at MTA-ELTE Lendület CMS Particle and Nuclear Physics Group, Eötvös Loránd University, Budapest, Hungary
32: Also at Wigner Research Centre for Physics, Budapest, Hungary
33: Also at IIT Bhubaneswar, Bhubaneswar, India
34: Also at Institute of Physics, Bhubaneswar, India
35: Also at Punjab Agricultural University, Ludhiana, India
36: Also at Shoolini University, Solan, India
37: Also at University of Hyderabad, Hyderabad, India
38: Also at University of Visva-Bharati, Santiniketan, India
39: Also at Indian Institute of Technology (IIT), Mumbai, India
40: Also at Deutsches Elektronen-Synchrotron, Hamburg, Germany
41: Also at Sharif University of Technology, Tehran, Iran
42: Also at Department of Physics, University of Science and Technology of Mazandaran, Behshahr, Iran
43: Now at INFN Sezione di Bari, Università di Bari, Politecnico di Bari, Bari, Italy
44: Also at Italian National Agency for New Technologies, Energy and Sustainable Economic Development, Bologna, Italy
45: Also at Centro Siciliano di Fisica Nucleare e di Struttura Della Materia, Catania, Italy
46: Also at Università di Napoli 'Federico II', Napoli, Italy
47: Also at Consiglio Nazionale delle Ricerche - Istituto Officina dei Materiali, Perugia, Italy
48: Also at Riga Technical University, Riga, Latvia
49: Also at Consejo Nacional de Ciencia y Tecnología, Mexico City, Mexico
50: Also at IRFU, CEA, Université Paris-Saclay, Gif-sur-Yvette, France
51: Also at Institute for Nuclear Research, Moscow, Russia
52: Now at National Research Nuclear University 'Moscow Engineering Physics Institute' (MEPhI), Moscow, Russia
53: Also at Institute of Nuclear Physics of the Uzbekistan Academy of Sciences, Tashkent, Uzbekistan
54: Also at St. Petersburg Polytechnic University, St. Petersburg, Russia
55: Also at University of Florida, Gainesville, Florida, USA
56: Also at Imperial College, London, United Kingdom
57: Also at P.N. Lebedev Physical Institute, Moscow, Russia
58: Also at Moscow Institute of Physics and Technology, Moscow, Russia
59: Also at California Institute of Technology, Pasadena, California, USA
60: Also at Budker Institute of Nuclear Physics, Novosibirsk, Russia

61: Also at Faculty of Physics, University of Belgrade, Belgrade, Serbia
62: Also at Trincomalee Campus, Eastern University, Sri Lanka, Nilaveli, Sri Lanka
63: Also at INFN Sezione di Pavia, Università di Pavia, Pavia, Italy
64: Also at National and Kapodistrian University of Athens, Athens, Greece
65: Also at Ecole Polytechnique Fédérale Lausanne, Lausanne, Switzerland
66: Also at Universität Zürich, Zurich, Switzerland
67: Also at Stefan Meyer Institute for Subatomic Physics, Vienna, Austria
68: Also at Laboratoire d'Annecy-le-Vieux de Physique des Particules, IN2P3-CNRS, Annecy-le-Vieux, France
69: Also at Şırnak University, Sirnak, Turkey
70: Also at Near East University, Research Center of Experimental Health Science, Nicosia, Turkey
71: Also at Konya Technical University, Konya, Turkey
72: Also at Piri Reis University, Istanbul, Turkey
73: Also at Adiyaman University, Adiyaman, Turkey
74: Also at Ozyegin University, Istanbul, Turkey
75: Also at Necmettin Erbakan University, Konya, Turkey
76: Also at Bozok Universitetesi Rektörlügü, Yozgat, Turkey
77: Also at Marmara University, Istanbul, Turkey
78: Also at Milli Savunma University, Istanbul, Turkey
79: Also at Kafkas University, Kars, Turkey
80: Also at Istanbul Bilgi University, Istanbul, Turkey
81: Also at Hacettepe University, Ankara, Turkey
82: Also at Istanbul University - Cerrahpasa, Faculty of Engineering, Istanbul, Turkey
83: Also at Vrije Universiteit Brussel, Brussel, Belgium
84: Also at School of Physics and Astronomy, University of Southampton, Southampton, United Kingdom
85: Also at Rutherford Appleton Laboratory, Didcot, United Kingdom
86: Also at IPPP Durham University, Durham, United Kingdom
87: Also at Monash University, Faculty of Science, Clayton, Australia
88: Also at Università di Torino, Torino, Italy
89: Also at Bethel University, St. Paul, Minneapolis, USA
90: Also at Karamanoğlu Mehmetbey University, Karaman, Turkey
91: Also at Bingol University, Bingol, Turkey
92: Also at Georgian Technical University, Tbilisi, Georgia
93: Also at Sinop University, Sinop, Turkey
94: Also at Erciyes University, Kayseri, Turkey
95: Also at Institute of Modern Physics and Key Laboratory of Nuclear Physics and Ion-beam Application (MOE) - Fudan University, Shanghai, China
96: Also at Texas A&M University at Qatar, Doha, Qatar
97: Also at Kyungpook National University, Daegu, Korea